OPERATING RISK ASSESSMENT OF MODERN POWER SYSTEM IN PRESENCE OF FLYWHEEL ENERGY STORAGE

A Thesis Submitted to the College of

Graduate and Postdoctoral Studies

In Partial Fulfillment of the Requirements

For the Degree of Master of Science

In the Department of Electrical and Computer Engineering

University of Saskatchewan

Saskatoon, Canada

By

Saket Adhikari

PERMISSION TO USE

In presenting this thesis in partial fulfilment of the requirements for a Postgraduate degree from the University of Saskatchewan, I agree that the Libraries of this University may make it freely available for inspection. I further agree that permission for copying of this thesis in any manner, in whole or in part, for scholarly purposes may be granted by the professor or professors who supervised my thesis work or, in their absence, by the Head of the Department or the Dean of the College in which my thesis work was done. It is understood that any copying or publication or use of this thesis or parts thereof for financial gain shall not be allowed without my written permission. It is also understood that due recognition shall be given to me and to the University of Saskatchewan in any scholarly use which may be made of any material in my thesis.

Requests for permission to copy or to make other use of material in this thesis in whole or part should be addressed to:

Head of the Department of Electrical and Computer Engineering
57 Campus Drive
University of Saskatchewan
Saskatoon, Saskatchewan S7N 5A9
Canada

OR

Dean
College of Graduate and Postdoctoral Studies
University of Saskatchewan
116 Thorvaldson Building, 110 Science Place
Saskatoon, Saskatchewan S7N 5C9
Canada

ABSTRACT

Stochastic perturbations in supply and demand during power system operations have always been a concern for power system operators and/or planners. These concerns have been aggravated in the past decade with large-scale integration of renewable energy sources (RES) such as wind and photovoltaics. The impacts of load fluctuations and/or random outages of major system components during the operation, such as loss of generating unit(s) and transmission line(s) are further aggravated due to increasing addition of intermittent RES in the system. Energy storage systems (ESS) can act as a buffer to maintain the supply-demand balance, and are therefore, gaining considerable attention in modern power system planning. It is important to have the ability to make quantitative assessment of associated risks in the system operation and to explore the potential of suitable resources such as ESS in mitigating these risks.

A reliability model of flywheel energy storage system (FESS) suitable for power system operational risk evaluation was developed in the research work presented in this thesis. Appropriate reliability assessment frameworks for different hierarchical levels of power system reliability evaluation were also introduced. The proposed frameworks and models were applied to the IEEE reliability test system and a modified Roy Billinton test system through several case studies.

This thesis presents a novel approach to quantify the impact of growing wind penetration on power system operational reliability and quantify the implications of implementing flywheel energy storage systems in mitigating these concerns. The work presented in this thesis provides methodology and indicators that will be valuable in developing operating policies for sustainable wind energy for the future.

ACKNOWLEDGEMENTS

I would like to express my earnest gratitude to my supervisor Dr. Rajesh Karki for his invaluable guidance and encouragement throughout this research work and in the preparation of this thesis. His pioneer ideas and extensive expertise were imperative to make my research meaningful and productive.

I appreciate the financial assistance provided by the college of graduate studies and research, the Department of Electrical and Computer Engineering and Natural Sciences and Engineering Research Council of Canada (NSERC) throughout my M.Sc. program.

I would like to sincerely thank Dr. Sherif O. Faried and Dr. Nurul A. Chowdhury for strengthening my knowledge on power systems through the related graduate courses. I am thankful to my colleagues: Mr. Prajjwal Gautam, Mr. Safal Bhattarai, Ms. Fang Fang and Mr. Damilola Fadele for their valuable help and suggestions throughout my research.

Last, but not the least, I would like to express my deepest gratitude to my parents for their constant support and encouragement.

TABLE OF CONTENTS

LIST OF TABLES

LIST OF FIGURES

LIST OF ABBREVATIONS

AGC	Automatic Generation Control
ARMA	Auto-Regressive Moving Average
BPS	Bulk Power System
COPT	Capacity Outage Probability Table
CWPD	Conditional Wind Power Distribution
CWSD	Conditional Wind Speed Distribution
DC-OPF	DC Optimal Power Flow
DOD	Depth of Discharge
ELD	Economic Load Dispatch
EPNS	Expected Power Not Served
ESS	Energy Storage System
EWS	Expected Wind Spillage
FESS	Flywheel Energy Storage System
FESU	Flywheel Energy Storage Unit
FUC	Fixed Unit Commitment
HL-I	Hierarchical Level I
HL-II	Hierarchical Level II
HL-III	Hierarchical Level III
IEEE-RTS	IEEE Reliability Test System
IWP	Initial Wind Power
IWS	Initial Wind Speed
LC	Load Curtailment
LOLE	Loss of Load Expectation
LOLEE	Loss of Energy Expectation
LPRR	Load Point Recovery Risk
MCO	Major Component Outages
M-RBTS	Modified Roy Billinton Test System
MT	Margin Time

MUC	Modified Unit Commitment
NERC	North American Electric Reliability Corporation
NREL	National Renewable Energy Laboratory
OPW	Operating Wind Penetration
ORR	Outage Replacement Rate
PCM	Power Control Module
PMSM	Permanent Magnet Synchronous Machine
RES	Renewable Energy Source
RM	Regulating Margin
RPS	Renewable Portfolio Standard
RR	Response / Recovery Risk
RRMF	Response Risk Multiplication Factor
SOC	State of Charge
SR	Spinning Reserve
SRR	System Recovery Risk
STC	Combination of Switchgear, Transformer and Cluster Controller
UCR	Unit Commitment Risk
WTG	Wind Turbine Generator

CHAPTER 1:INTRODUCTION

1.1. Power System Reliability

The ability of a power system to provide the electric supply to their customers with satisfactory quality and continuity is perceived as its reliability in a general sense. Typically, a power system consists of generation, transmission and distribution facilities in order to generate and deliver the required electric energy to customers connected at the load points. As reliable power supply is an important prerequisite of a modern economy, electric power utilities have invested heavily in key power system sectors to meet their customer demands economically, while maintaining an acceptable level of reliability. Owing to the random failure of different components within the system, no power system can be made perfectly reliable. A high assurance of the continuity of electric power supply calls for proper reliability centered design, planning, operation and maintenance, which ultimately results in increased investment. An increase in system reliability is generally achieved through increased investment. However, at some point the additional investment in infrastructures does not yield a justifiable improvement in reliability. Therefore, power system reliability assessment is important and useful in arriving at an optimal investment decision for acceptable level of reliability.

The term ‘reliability’ in the context of power system is very broad and covers a host of sub-categories. The overarching concept of power system reliability can be sub-divided into two fundamental areas [1] as shown in Figure 1.1.

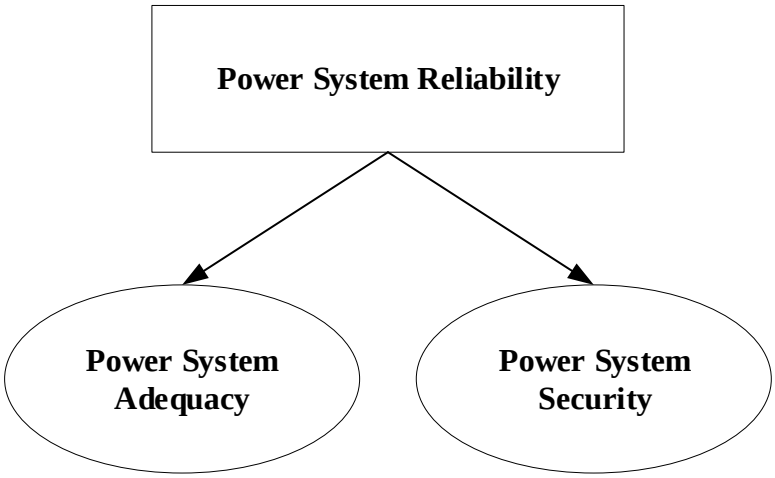

Figure 1. 1. Sub-division of power system reliability.

1.1.1. Power System Adequacy and Security

Power system adequacy deals with sufficiency of generation, transmission and distribution facilities to make electrical energy available at the customer load points. Adequacy assessment does not account for different kinds of perturbations within the system but is rather limited to static conditions of the system primarily considered during the system planning phase. System security, on the other hand, is concerned mostly with the dynamic behavior of the system. Specifically, security assessment deals with the ability of existing resources to respond to disturbances within definite time-frame. The disturbances could be both local and wide-spread and include loss of generation and transmission facilities. It is the role of a system operator to maintain the security of the system by making an informed decision based on appropriate security assessment.

It is thus clear that adequacy and security encompasses two different aspects of power system reliability evaluation. The loss of load expectation (LOLE) and the loss of energy expectation (LOEE) are commonly preferred measure of reliability in the system adequacy domain [2, 3], while operating risk assessment, usually via unit commitment risk (UCR) and response risk (RR) analysis, falls under system security assessment which also directs the scope of this thesis.

1.1.2. Functional Zones and Hierarchical Levels

Three basic functional zones, namely generation, transmission and distribution system constitute a physical framework for power system reliability evaluation. The combination these functional zones forms the three hierarchical levels in the reliability evaluation, as shown in Figure 1.2. However, it should be noted that the reliability assessment can be performed within each of the individual functional zones. Hierarchical level I (HL I) refers to the reliability assessment considering only the generation facility. Under HL I evaluation, transmission and distribution facilities are not considered. Hierarchical level II (HL II) evaluation, on the other hand, accounts for the transmission and generation systems. The transmission line constraints and location of the generation resources and the load points are additional complexities inherent in HL II evaluation. Hierarchical level III (HL III) brings all the functional zones into the evaluation framework. As the size of a physical system ascends from HL I to HL III, so does the complexity in the reliability evaluation. Being the most basic form of reliability evaluation, a considerable amount of work has been done in the past on HL I study compared to the other two hierarchical levels. The research work presented in this thesis was carried out both at the HL I and HL II levels. The progression of the study from one hierarchical level to the other is further explained towards the end of this chapter in Section 1.6.

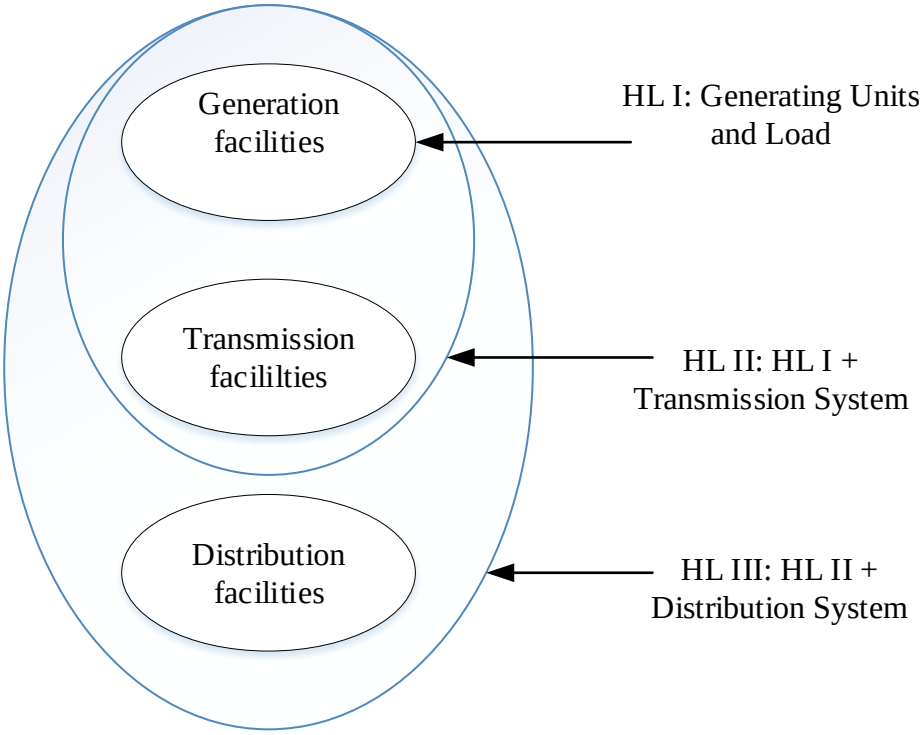

Figure 1. 2. Functional zones and hierarchical levels in reliability evaluation.

1.2. Power System Operation and Operational Reliability

The stochastic nature of perturbations within the system as a result of random failure of the system components and/or load and generation fluctuations have always been posing challenges to system operators in maintaining continuous supply of electric power to the customers. Based on short-term forecasts of the load, a certain number of units are committed to meet the forecast load in the given time. To compensate for any unforeseen disturbance that may arise during system operation, the units are committed in such a way that the total capacity exceeds the forecast demand by a reserve margin. A committed unit that is dispatched to take a load less than its rated capacity carries a as spinning reserve [4] which is ready to take up the load if needed. . There are various means of enhancing the spinning reserve with other types of reserves, such as rapid start units, hot reserves, assistance from interconnected systems, voltage/ frequency reduction etc. [1]. The spinning reserve and the additional means of its enhancement are collectively known as operating reserve.

At the event of a contingency resulting in a power deficit, the system inertia tries to compensate for the generation drop by slowing down the rotational speed of synchronous machines [5]. In such situations the operating reserve needs to respond immediately following the contingency to restore the nominal frequency within a very small time-frame in order to prevent further catastrophic consequences. The fraction of operating reserve which is available within a short margin - time is commonly known as the regulating margin [6].

It is apparent that two major aspects of reliable power system operation are unit commitment decision and operating reserve allocation. The common practice in utilities is to use deterministic approach in unit commitment which considers largest unit as the operating reserve. However, this approach can sometimes lead to over-scheduling of the generation units which is ultimately a cost burden and sometimes lead to under-scheduling of the generation units that results in operating cost reduction at the expense of poor reliability. This inconsistency in risk evaluation can be overcome to a great extent by applying probabilistic techniques. A large volume of literatures [7-13] can be found in the area of probabilistic risk assessment. The most commonly used risk indices in probabilistic operational risk assessment are UCR and RR [4]. UCR is concerned with the decision of the appropriate number of units to be committed in any given time such that risk of failing to meet the load is within acceptable range, while RR is associated with allocating appropriate reserve margin in the committed units in order to compensate for any unforeseen disturbances that may arise during system operation. The scope of this thesis is limited to the RR domain.

1.3. Role of Energy Storage Systems in Power System Operation with Large-scale Wind Integration

1.3.1. Impacts of Increased Wind Penetration in Power System Operation

Conventional fossil fuel fired thermal generation systems are known to be significant contributor of greenhouse emission. In addition to the safety concern associated with nuclear energy, the depletion of limited stock of fossil fuel has been pressurizing the nations around the

globe to resort toward the renewable energy sources (RES). To this end, many countries have agreed to renewable portfolio standard (RPS). RPS is the commitment to meet the definite share of national generation mix by RES within a certain time frame. In past decade wind energy has emerged as a promising dominant renewable source. Wind power already supplies a large share of the electricity in Denmark, Germany, and Spain and is continually growing. The advent of efficient technologies associated with wind power and reduction in their price together with government incentives and the high cost of fossil fuels have collectively caused the wind energy to have a promising future in the global energy market [14]. More than 54000 MW of wind power was installed across the global market in 2016 alone. As of December 2016, the installed wind capacity in Canada was 12239 MW which accounts for around 6% of Canada's electricity demand [15]. The present situation of the generation mix can still be considered as safe from reliable system operation point of view. However, the global trend of wind power growth, such as shown in Figure 1.3, is raising concerns among power system operators regarding the reliability of system operation.

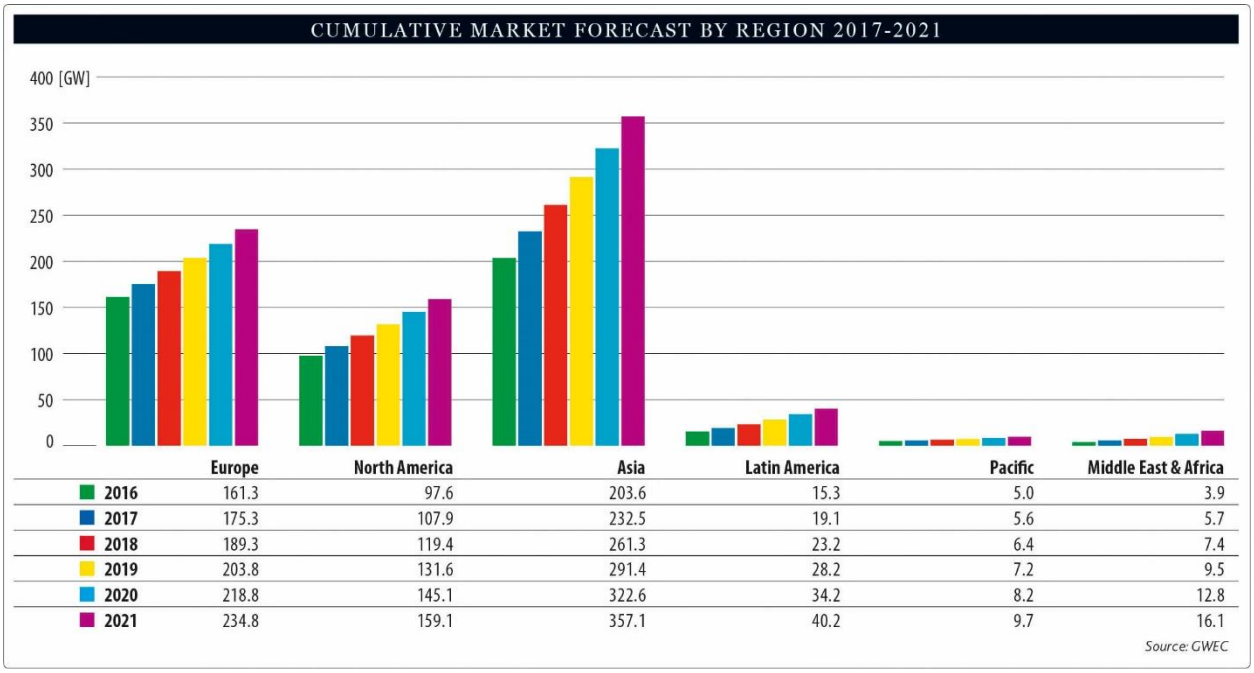

	Europe	North America	Asia	Latin America	Pacific	Middle East & Africa
2016	161.3	97.6	203.6	15.3	5.0	3.9
2017	175.3	107.9	232.5	19.1	5.6	5.7
2018	189.3	119.4	261.3	23.2	6.4	7.4
2019	203.8	131.6	291.4	28.2	7.2	9.5
2020	218.8	145.1	322.6	34.2	8.2	12.8
2021	234.8	159.1	357.1	40.2	9.7	16.1

Figure 1. 3. Cumulative market forecast for wind power by region, 2017 – 2021 [16]

Intermittency and uncertainty associated with the wind power has increased challenges in maintaining the system reliability in wind-integrated power systems. The output of conventional

generation sources can be controlled to meet the load in specified time. Wind power generation, on the other hand, cannot be controlled and dispatched in conventional sense due to site-specific stochastic nature of wind speed. System operators dispatch the committed units to meet the load at any specified time and, while doing so, a small fraction of operating reserve is left in the dispatched units. With the increment in operating wind penetration, the share of firm generation is reduced and the system gradually loses the inertial response. The reduced inertial response and increased variability and uncertainty in the system operation due to the addition of intermittent energy sources put the system operation in significant operating risk. This entails that additional operating reserve is necessary to compensate for the increased variability and uncertainty in the system operation.

1.3.2. Energy Storage System in Wind-Integrated Power System

It has been established in the previous section that the integration of intermittent energy sources such as wind power introduces challenges to the system operator to maintain the acceptable reliability in system operation and calls for additional provision to enhance the effective-operating reserve in the system to cope with the increased uncertainty. Energy storage system (ESS) can mitigate the generation variability and moderate the transmission congestion thereby improving the operating reliability and enabling the further penetration of RES [17, 18]. It is therefore there is growing research interest in the application of ESS in wind-integrated power system [19-23]. ESS serves as a buffer maintaining balance between electric power and demand. In addition to adding flexibility to the power system thereby increasing grid's capability to allow larger penetration of intermittent energy sources, ESS also enhances the grid's resiliency to power outages resulting from severe weather events and attacks on the cyber-physical systems [24-27].

A host of ESS technologies are emerging in present time and their suitability within the power system application varies greatly depending upon their inherent characteristics such as energy density, power density, useful life, efficiency, depth of discharge, etc. Batteries, fuel cells, compressed air energy storage and flywheels are some commonly used ESS in power system applications. The literature [28] gives an oversight of different energy storage technologies, their evolution over time and future prospect. The characteristics of different ESS and their suitability

in various aspects within power system is discussed in [29]. Tables 1.1 and 1.2 shows the characteristics and prospective applications of several ESS power system.

Table 1. 1. Characteristics of different energy storage technologies [29].

S.N.	Energy Storage Technology	Discharge Duration (hours)	Response Time
1	Pumped Hydro	8 to 10	minutes
2	Compressed Air	8 to 10	minutes
3	Flywheel	0.03 to 1	milliseconds
4	Advanced Lead Acid Battery	2 to 5	milliseconds
5	Lithium Ion Battery	1 to 4	milliseconds

Table 1. 2. Power system application of different energy storage technologies [29], [30]

Application	ESS Options
Regulation Renewable Energy Smoothing	Flywheels Lithium Ion Battery NaS Battery
Renewable Capacity Firming Load Following Energy Time Shifts Renewable Energy Time Shifts	Pumped Hydro Compressed Air NaS Battery Lithium Ion Battery

Long-term storage technologies such as pumped hydro and compressed air can support for several hours to days with below-average renewable generation [31] and thus are suitable for renewable capacity firming, load levelling and energy time shift. On the other hand, there might be situations where large amount of power is needed immediately but for short durations. The NERC standards, for instance, require that an immediate response should be available through automatic generation control (AGC) to maintain frequency and tie line regulation and the contingency reserve should be able to restore the system to its pre-disturbance state within 15

minutes [32]. To ensure such a prompt assistance in case of unforeseeable events during operation such as restoring power balance in the event of major contingencies to maintain the system security, an ESS with fast response capability such as flywheel energy storage systems (FESS), batteries and ultra-capacitors are needed. Although it is comparatively a less mature technology, FESS outranks other ESS in terms of lesser environmental impact, longer lifespan, and high depth of discharge and low maintenance requirements. Despite several technological difficulties in the past, the recent improvement in power electronics, bearing system and rotor materials needed for high speed flywheels has opened new possibilities for FESS to be used for improving power system operating risk. Reliability modelling of FESS and investigation of its potential in terms of its operational reliability benefits in power system operation with a large-scale wind integration forms the major focus of this thesis.

1.4. Flywheel Energy Storage System

A flywheel is a mechanical device which stores energy in rotational form. The rotational speed dictates the amount of energy stored, which is known as state of charge (SOC). Although the technology itself in the field of power system is not mature, flywheel as a means of mechanical energy storage systems has existed for thousands of years [31]. The potter's wheel, for instance, is one of the earliest applications of flywheel [32].

In the context of power system applications, the flywheel energy storage system (FESS) consists of a group of flywheels with other essential power electronic components. FESS stores the energy in the form of kinetic energy of a rotating disc which can be extracted as needed through the combination of electrical generator and power converter, and vice versa. While the fundamental idea of using a FESS for grid application is not new, the technology did not see much improvements for quite some time. However, with recent development of solid-state power electronics, magnetic bearings and construction materials, the FESS has shown a potential for grid-scale application. New market policies and tariffs that allow new technologies to compete in the market, have been issued or are in the process of being issued [33] and have further secured the economic viability of expensive emerging technology such as FESS. There are many grid-scale FESS plants currently in operation in many parts of North America, such as the 3 MW plant at Tyngsboro, Massachusetts and the 20 MW facility at Stephentown, New York. A response time

of fraction of seconds, a life span of 20 years with no degradation, 100% depth of discharge (DOD), hundreds of thousands of full DOD cycles, exceptionally high permissible rotating speed, scalable design to meet almost any power requirements are the advantageous features of the commercially available grid-scale flywheels [34].

The major components of a flywheel energy storage unit (FESU) are the cooling system, bearing system, motor / generator, rotor drum, vacuum enclosures, and power electronics unit As depicted in Figure 1.4 and Figure 1.5 [34]. The rotor drum is the essential component of the FESU whose rotational speed determines the amount of energy stored in the unit, also known as state of charge (SOC), as expressed in (1.1). The energy density, δ [35] of a FESU can be expressed as in (1.2). From (1.2) it is clear that the maximum energy that can be stored is driven by the permissible speed of rotation and the ratio of moment of inertia to mass, (I/m) which depends on material properties of rotor. The material properties of the rotor is again one of the key factors to determine the permissible speed of the rotor since the chances of rotor failure becomes significantly higher at higher speed [35]. It thus becomes important to analyze the implication of the increased of failure rate in the reliability of the FESU, as will be done in subsequent chapter.

$$SOC = \frac{1}{2} I\omega^2 \qquad (1.1)$$

$$\delta = \frac{1}{2} \frac{I}{m} \omega^2 \qquad (1.2)$$

Where,

'I' is mass moment of inertia in kg-m^2, ω the rotational speed in rad/s and 'm' is mass in kg.

A generator is coupled with a rotor drum for energy conversion from rotational form to electrical form and vice versa. The machine is operated in both the motor and generator mode depending upon the need. A permanent magnet synchronous machine (PMSM) is commonly preferred in a FESS for its efficiency, while variable reluctance machines and asynchronous machines are also used as generator / motor in FESS [36]. The rotor is supported by magnetic bearings and is enclosed in a vacuum enclosure to provide a near-frictionless environment. A dedicated cooling system becomes very important to dissipate the heat developed during the operation, since the entire operation takes place inside the vacuum where heat dissipation becomes challenging. The power converter (usually a back-to-back converter) is used to make the power exchange between the grid (or the external system) and FESU. A power control module keeps

track of SOC and state of health of the associated FESU. It receives the operational signal and drives the power converter to make the power exchange [34].

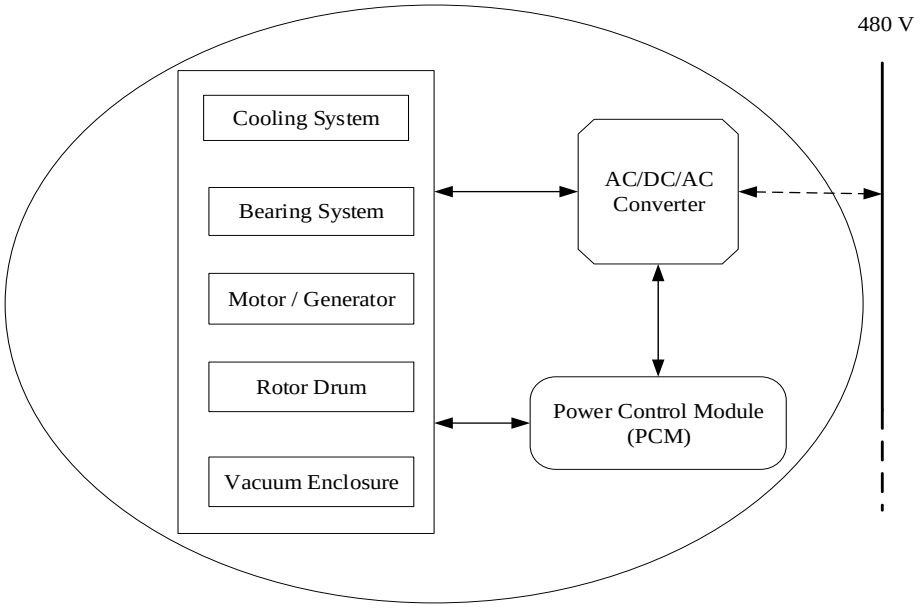

Figure 1. 4. Block-diagram representation of a typical flywheel energy storage unit.

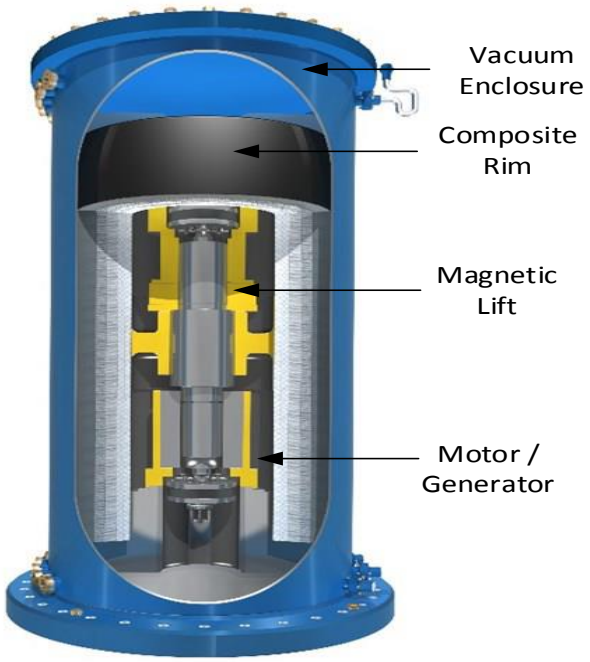

Figure 1. 5. A schematic of a commercial flywheel energy storage unit [34].

A typical FESS plant consists of a large fleet of FESUs arranged in multiple clusters as shown in Figures 1.6 and 1.7. The modular arrangement minimizes the plant's footprint and increases the plant's availability. It also adds scalability of the storage system in order to meet the required power and energy demand.

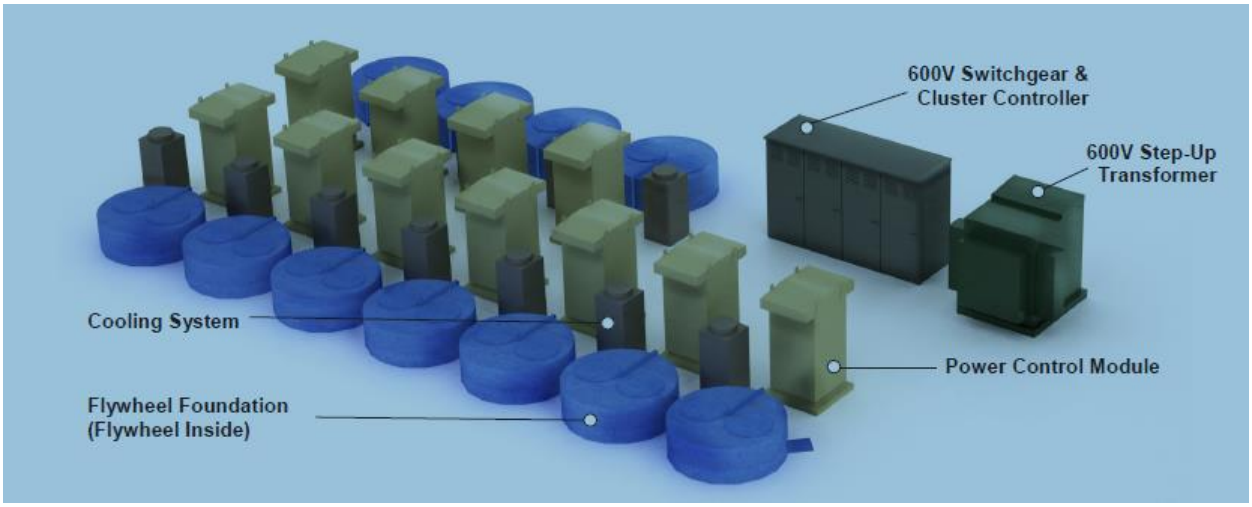

Figure 1. 6. A schematic of a flywheel cluster in a typical FESS plant [34].

Figure 1. 7. A schematic of a typical FESS plant [34].

1.5. Problem Statement and Research Objectives

It is the responsibility of a power system operator to continuously balance the supply and demand of energy amidst the uncertainties in supply and demand variations that prevail randomly and continuously in time. Therefore, the important tasks in the power system operation are: (i) deciding the number of committed units based on the load forecasted for the time of interest and (ii) allocating sufficient operating reserve. For a given load, the system operators commit a fixed number generating units and determine an economic schedule of the committed units to meet the load. The scheduling of the committed units should ensure an acceptable level of reliability with regard to probable disturbances while maintaining the economics of operation. It thus becomes the responsibility of a system operator to find a proper trade-off between 'operational reliability' and 'economics'.

The most commonly used approach to assess the amount of operating reserve during unit commitment is the N-1 approach. In this method, an operating reserve equal to largest generating unit is required to withstand the worst case disturbance scenario resulting from the forced outage of the largest committed generating unit. The deterministic way of unit commitment such as N-1 approach, however, undermines the stochastic behaviors of the committed units, transmission line outages, as well as other power system variables such as random wind and load variations. The

approach, in some cases, results in over commitment of generating units which might make the system operation more reliable but at the expense of high operational cost. The same approach in some other cases, yields under-commitment of resources which apparently saves operational cost but severely jeopardize the operational reliability. A notable number of literatures on probabilistic approach of power system operating risk assessment can be found in [37], which address the issues raised earlier in the deterministic approach. Despite of the inconsistency in operating risk profile as offered by deterministic approach, the "N-1" criterion is still preferred by many utilities because of its simplicity of application. This criterion will face increasing problems as wind power penetrations increase in power systems.

The scheduling of the committed units to meet system load determines the amount of available operating reserve. This is another important responsibility of the system operator, since the amount of operating reserve is mainly responsible for mitigating any disturbances during system operation. The economic load dispatch (ELD) is commonly used in practice to determine loading schedule of the committed units. The ELD tries to minimize the cost of operation. However, methodologies based on ELD do not incorporate the need to maintain a reasonable level of operating reliability. Several works have been done in the past to develop appropriate methodologies to assess the operating risk associated with the dispatch decision of the committed generating units having various capacities and ramping abilities. The probability of failing to provide sufficient generation response within a certain time following a major contingency disturbance during the system operation is known as the response risk (RR) [38]. Reference [4] proposed a method to evaluate the response risk associated with a dispatch decision. The method uses capacity outage probability table (COPT) constructed using the outage replacement rate (ORR) of the committed units which are carrying the spinning reserve. The methodology implicitly makes an assumption that only the units with spinning reserve are exposed to failure. And thus, only these units are used in evaluating the generation response needed within a specified time, also known as margin time (MT). Furthermore, when these units carrying the spinning reserve like any other committed units fail, they introduce new disturbance in the system in addition to the original disturbance to which the units are responding. Apparently, this additional disturbance further limits the ability of the available committed units to respond to the disturbance. These two limitations necessitate the development of a new evaluation framework for better appraisal of the response risk associated with the dispatch decision.

The uncertainty and intermittency of wind power has further added new challenges for system operator in maintaining the economic and reliable operation of power system with large scale wind integration. The stochastic nature of wind power adds the element of uncertainty in the power system which already has stochastic element such as random failure of generating unit, lines and load fluctuation. The random behavior of latter part can be at least compensated to some extent due to controllability offered by the conventional generation source. But the same cannot be expected in case of wind power, unless one has suitable means of storing energy for future usage. The ability of the operating system to respond toward a contingency such as sudden loss of a line or a generating unit is likely to be inhibited by the wind power fluctuations within the margin time following the contingency. It should, however, be noted that the availability of surplus wind power could add to the response capacity of the operating system. It is therefore the short-term wind power model incorporating the diurnal characteristics of wind speeds is essential in the power system operating risk analysis for more accurate assessment of the impacts of wind penetration in the system operation. The allocation of operating reserve becomes a more important consideration with large amount of wind power in the system operation. The larger the operating wind penetration, the bigger is the uncertainty in system operation and larger is the operating reserve needed to ensure the reliable operation. The past works on security domain of system reliability of wind-integrated power system, as mentioned earlier, mostly suggest modifying the economic dispatch based on response risk criterion and, if needed, adding more of the conventional units. With the operating wind penetration level that forms a significant portion of the load, the risk-constrained dispatch might not be always a viable option. In particular, if the needed additional regulation reserve comes from a conventional energy source, the environmental incentive which is the major driving force for resorting to the renewable energy source (RES) will be compromised. As discussed in sections 1.3.2 and 1.4, energy storage system with fast ramping abilities such as flywheel energy storage system (FESS) thus have potential to be useful in maintaining the operating reliability of the modern power system. To this regard, the probabilistic framework for the quantitative risk assessment of the modern power system operation, incorporating probabilistic models of wind power and the energy storage system is very important.

Reported works on FESS [39- 44] are mainly focused on comparative advantages, suitability in different applications and / or the design and loss analysis of FESS, and lack the direct-usability in the quantitative risk assessment of the power system operation. Developing a probabilistic

model of FESS suitable for the risk evaluation of the power system operation and to quantify the operational reliability benefits of FESS in wind-integrated power system operation are two of the major objectives of this research work. To quantify the impacts of increasing operating wind penetration in the operating reliability of the system, through appropriate short-term wind power models is an equally important objective of this research work. In contrast to traditional approaches of response risk analysis which are focused on 'generation response' on hierarchical level I, creating an analytical framework for operating risk assessment of composite power system is an important task of this research.

Two general objectives of the present work are:

- To quantify the impact of increasing operating wind penetration on reliability of the system operation.
- To quantify the reliability benefits of FESS in power system operating reliability.

The specific objectives of this research work include:

- To develop a probabilistic model of FESS incorporating its charging/discharging and failure characteristics, suitable for application in quantitative risk assessment of power system operation.
- To develop an improved analytical framework for operating risk assessment of the wind-integrated power system.
- To develop short term time-dependent disturbance model incorporating the uncertainty in wind power, load variation and random forced outages of committed generating units.
- To extend the fundamental concept of 'response risk' analysis used in hierarchical level I, in terms of 'recovery risk' analysis of individual bulk load delivery points to address the locational impact of operational disturbances.

1.6. Organization of Thesis

This thesis is written in manuscript style and contains five chapters altogether. Excluding Chapter 1 and Chapter 5, which are introductory and concluding chapters of this thesis, remaining three chapters are preceded by a preface to the corresponding chapter. The preface is aimed to

provide more general view of immediately following chapter and explain how does it tie up to the central theme of the thesis.

Chapter 1 is introductory portion of thesis and provides an overview of power system reliability evaluation and its necessity in the context of growing global consumption of renewable energy. The chapter builds up on the role of energy storage technologies from operating risk perspective of power system operation with large-scale wind integration. Furthermore, Chapter 1 presents a brief introduction of flywheel energy storage system (FESS) and lays down the scope and the objectives of the research work presented in this thesis.

Reliability modelling of flywheel energy storage system suitable for power system operational risk assessment is presented in Chapter 2. The impacts of failure rates of critical components of FESS and the length of operational mission times on state of charge (SOC) model are investigated in this chapter.

Chapter 3 presents the novel framework for evaluation of power system operating risk and quantifies the impact of increasing operating wind penetration. Also, it quantifies the reliability benefits of using FESS in wind-integrated power system. The operating reliability evaluation presented in this chapter falls under hierarchical level I.

Chapter 4 extends the fundamental idea of generation response risk to incorporate the transmission system network into operating risk evaluation. A methodology for operating risk analysis of bulk power system (BPS) is presented in this paper. The methodology is suitable for quantifying the reliability benefits of FESS from operating risk perspective of BPS operation.

Chapter 5 summarizes the overall research work. The general conclusions from application of proposed methodologies through various studies carried out in different chapters of the thesis are presented in this chapter.

1.7. References

[1] R. Billinton and R. N. Allan, "Power-system reliability in perspective," Electronics and Power, vol. 30, pp. 231-236, 1984.

[2] Billinton, R., "Criteria used by Canadian utilities in the planning and operation of generating capacity", *IEEE Transactions on Power Apparatus and Systems*, Vol. 3, No. 4, pp. 148801493, November 1988

[3] Billinton, R., Allan, R. N., Reliability Assessment of Large Electric Power Systems, Kluwer Academic Publishers, Boston, USA, 1988.

[4] R. Billinton and R. N. Allan, Reliability Evaluation of Power Systems. New York: Plenum, 1996.

[5] National Renewable Energy Laboratory (NREL), "Operating reserves and variable generation", Technical Report, NREL/TP-5500-51978, 2011.

[6] W. Stadlin, "Economic allocation of regulating margin", *IEEE Transactions on Power Apparatus and Systems*, pp. 1776-1781, July 1971.

[7] G. Calabrese, "Generating reserve capacity determined by the probability method," *American* Institute of Electrical Engineers, Transactions of the, vol. 66, pp. 1439-1450, 1947.

[8] R. Billinton, *Power System Reliability Evaluation*. Gordon and Breach Science Publishers. Science Pub (1970): 92-118.

[9] R. N. Allan, R. Billinton, A. M. Breipohl and C. H. Grigg, "Bibliography on the application of probability methods in power system reliability evaluation: 1987-1991," *IEEE Transactions on Power Systems*, vol. 9, pp. 41-49, 1994.

[10] R. Billinton and R. N. Allan, *Reliability Evaluation of Power Systems*. Pitman Books, 1984.

[11] Power System Engineering Committee, "Bibliography on the Application of Probability Methods in Power System Reliability Evaluation 1971-1977," *IEEE Transactions on Power Apparatus and Systems*, vol. PAS-97, pp. 2235-2242, 1978.

[12] R. Billinton, R. N. Allan and L. Salvaderi, Applied reliability assessment in electric power systems. 1991.

[13] R. N. Allan, R. Billinton, S. M. Shahidehpour and C. Singh, "Bibliography on the application of probability methods in power system reliability evaluation: 1982-7," *IEEE Transactions on Power Systems*, vol. 3, pp. 1555-1564, 1988.

[14] P. Fairley, "Can wind energy continue double-digit growth?," in *IEEE Spectrum*, vol. 45, no. 2, pp. 16-16, Feb. 2008.

[15] [http://canwea.ca/wind-energy/installed-capacity/, accessed 10/2017].

[16] Global Wind Energy Council, Global Wind Report Annual Market Update 2015, Wind energy Technol., pp. 1–76, 2015.

[17] J. Cui, K. Li, Y. Sun, Z. Zou and Y. Ma, "Distributed energy storage system in wind power generation," *2011 4th International Conference on Electric Utility Deregulation and Restructuring and Power Technologies (DRPT)*, Weihai, Shandong, 2011, pp. 1535-1540.

[18] Rick Miller, "Wind integration utilizing pumped storage," *Platts 2nd Annual Power Storage*, February 8-9, 2010.

[19] J. Shi, W. J. Lee and X. Liu, "Generation scheduling optimization of wind-energy storage system based on wind power output fluctuation features," *IEEE Transactions on Industry Applications*, vol. 54, no. 1, pp. 10-17, Jan.-Feb. 2018.

[20] H. Zhao, Q. Wu, and S. Hu, "Review of energy storage system for wind power integration support," *Appl. Energy*, vol. 137, pp. 545–553, 2015.

[21] Y. Luo and D. Li, "A model predictive control method of battery energy storage for smoothing wind power fluctuation," Elect. Power Sci. Eng., vol. 31, pp. 1–6, 2015.

[22] G. Yan, S. Feng, and J. H. Li, "Review on combined wind power generation and energy storage systems," *Energy Storage Sci. Technol.*, vol. 3, pp. 297– 301, 2014.

[23] D. Francisco, S. Andreas, G. Oriol, "A Review of energy storage technologies for wind power applications," *Renew. Sustain. Energy Rev*., vol. 16, pp. 2154–2171, 2012.

[24] G. Papaefthymiou, K. Grave, and K. Dragoon, "Flexibility options in electricity systems," ECOFYS Leonardo Energy, Berlin, Germany, Tech. Rep. POWDE14426, Mar. 2014.

[25] M. G. Molina, "Energy storage and power electronics technologies: A strong combination to empower the transformation to the smart grid," in *Proceedings of the IEEE*, vol. 105, no. 11, pp. 2191-2219, Nov. 2017.

[26] B. Singh, P. Roy, T. Spiess, and B. Venkatesh, "Achieving electricity grid resiliency," Centre Urban Energy, Toronto, ON, Canada, White Paper, Oct. 2015.

[27] H. Kondziella and T. Bruckner, "Flexibility requirements of renewable energy based electricity systems—A review of research results and methodologies," *Renew. Sustain. Energy Rev.*, vol. 53, pp. 10–22, Jan. 2016.

[28] M. S. Whittingham, "History, Evolution, and Future Status of Energy Storage," *in Proceedings of the IEEE*, vol. 100, Special Centennial Issue, pp. 1518-1534, May 13 2012.

[29] K. S. Tam, "Energy storage technologies for future electric power systems," *10th International Conference on Advances in Power System Control, Operation & Management (APSCOM 2015)*, Hong Kong, 2015, pp. 1-6.

[30] [https://www.tesla.com/en_CA/blog/Tesla-powerpack-enable-large-scale-sustainable-energy-south-australia, accessed 5/2018]

[31] M. E. Amiryar and K. R. Pullen, "A review of flywheel energy storage system technologies and their applications," Applied Sciences, vol. 7, no. 3, 2017.

[32] Genta, G, Kinetic Energy Storage: Theory and Practice of Advanced Flywheel Systems. Butterworth Heinemann Ltd.: London, UK, 1985.

[33] M. L. Lazarewicz and T. M. Ryan, "Integration of flywheel-based energy storage for frequency regulation in deregulated markets," *IEEE PES General Meeting*, Minneapolis, MN, 2010, pp. 1-6.

[34] [http://beaconpower.com/wp content/themes/beaconpower/inc/beacon_power_brochure_081414.pdf., accessed: 8/2016]

[35] Y. Bai, Q. Gao, H. Li, Y. Wu, and M. Xuan, "Design of composite flywheel rotor," Front. Mech. Eng. China, vol. 3, no. 3, pp. 288–292, 2008.

[36] R. Sebastián and R. Peña Alzola, "Flywheel energy storage systems: Review and simulation for an isolated wind power system," *Renew. Sustain. Energy Rev.*, vol. 16, no. 9, pp. 6803–6813, 2012.

[37] M. T. Schilling, R. Billinton and M. G. dos Santos, "Bibliography on power systems probablistic security analysis 1968-2008," *International Journal of Emerging Electric Power Systems*, vol. 10, May 2009.

[38] A.V.Jain and R.Billinton, "Spinning reserve allocation in a complex power system," in *IEEE Winter Power Meeting*, New York, N.Y., 1973, C 73 097-3, pp. 1-8.

[39] X. Zhang and J. Yang, "A DC-link voltage fast control strategy for high-speed PMSM/G in flywheel energy storage system", *IEEE Transactions on Industry Applications*, vol. PP, no. 99, pp. 1-1.

[40] R. Hebner, J. Beno, and A. Walls, "Flywheel batteries come around again", *IEEE spectrum*, vol. 39, no. 4, pp. 46–51, 2002.

[41] S. Vazquez, S. M. Lukic, E. Galvan, L. G. Franquelo and J. M. Carrasco, "Energy storage systems for transport and grid applications", *IEEE Transactions on Industrial Electronics*, vol. 57, no. 12, pp. 3881–3895, 2010.

[42] M. Farhadi and O. Mohammed, "Energy storage technologies for high-power applications", *IEEE Transactions on Industry Applications*, vol. 52, no. 3, pp. 1953-1961, May-June 2016.

[43] M. I. Daoud, A. S. Abdel-Khalik, A. Massoud, S. Ahmed and N. H. Abbasy, "On the development of flywheel storage systems for power system applications: A survey", *2012 XXth International Conference on Electrical Machines*, Marseille, 2012, pp. 2119-2125.

[44] B. H. Kenny, P. E. Kascak, R. Jansen, T. Dever and W. Santiago, "Control of a high-speed flywheel system for energy storage in space applications", *IEEE Transactions on Industry Applications*, vol. 41, no. 4, pp. 1029-1038, July-Aug. 2005.

[45] F. Deiana, A. Serpi, J. Abrahamsson, I. Marongiu and G. Gatto, "Extensive losses estimation of a novel high-speed permanent magnet synchronous machine for flywheel energy storage systems", *2016 XXII International Conference on Electrical Machines (ICEM)*, Lausanne, 2016, pp. 1728-1734.

[46] C. Zhang, K. J. Tseng, T. D. Nguyen and S. Zhang, "Design and loss analysis of a high speed flywheel energy storage system based on axial-flux flywheel-rotor electric machines", *2010 Conference Proceedings IPEC*, Singapore, 2010, pp. 886-891.

PREFACE TO CHAPTER 2: RELIABILITY MODELLING OF FLYWHEEL ENERGY STORAGE SYSTEM FOR POWER SYSTEM OPERATIONAL RELIABILITY ASSESSMENT

The manuscript entitled "Reliability Modelling of Flywheel Energy Storage System for Power System Operational Reliability Assessment" is presented as Chapter 2. The manuscript has been submitted and accepted for presentation in SEEP 2018 11th International Conference on Sustainable Energy and Environmental Protection. The basics of reliability modelling of flywheel energy storage system considering its suitability in power system operational risk assessment are presented in this chapter. The work presented in Chapter 2 addresses the first objective of the research which is developing a reliability model of flywheel energy storage system suitable for quantitative risk assessment of the power system operation.

CHAPTER 2:RELIABILITY MODELLING OF FLYWHEEL ENERGY STORAGE SYSTEM FOR POWER SYSTEM OPERATIONAL RELIABILITY ASSESSMENT

Saket Adhikari and Rajesh Karki

2.1. Abstract

Reliable and economic operation of power systems face extreme challenges in integrating large scale renewable energy sources due to intermittency and uncertainty in their power generation. It is therefore important to make quantitative risk assessment and explore potential resources to mitigate such risks. A probabilistic model of flywheel energy storage system (FESS) incorporating its specific charge/discharge, performance and failure characteristics, suitable for power system operational risk assessment is presented in this paper. The methodology used in the modelling offers flexibility to accommodate different plant configurations and is applied to illustrate comparative analysis of two typical FESS topologies. The impacts of failure rates of the critical components of a FESS on its expected state of charge (SOC) and its probabilistic capacity model during operation is illustrated. The impacts of the length of operational mission times on the SOC model are also investigated. The application of proposed model is demonstrated by assessing its ability to respond to disturbances from sudden wind and load changes on a test system.

2.2. Introduction

The growth in renewable energy in electric power systems in the last decade indicates a promising future for renewable energy. Many countries have already agreed to implement policy such as the Renewable Portfolio Standards (RPS) and some are in the process of implementing it.

RPS is a commitment to produce a certain percentage of the total generation using renewables within a specified time-frame [1]. In 2015, almost fifty percent of the global energy

growth came from wind generation alone. It is estimated that a total of USD 3.6 trillion will be invested in wind power between 2014 and 2040 [2]. Wind power is apparently the most preferred renewable energy source (RES) for bulk power production and is likely to be a mainstream source of energy in the near future. The intermittency and uncertainty inherent in RES pose significant threat to power system reliability during normal operation and during contingencies [3-5]. With rapid increase in RES penetration in power systems throughout the world, system operators are becoming increasingly concerned with their impacts on reliable and economic system operation. Energy storage systems (ESS) can effectively contribute to maintain the balance in supply and demand of energy and thus ensure reliable operation. ESS provide some degree of controllability to these stochastic energy sources.

The knowledge of the operating risks associated with potential contingencies of varying magnitudes during a system operating scenario will help system operators make an informed decision. The probabilistic risk assessment becomes inevitable in wind-integrated system planning and operation when a large portion of the generation mix is intermittent and stochastic in nature. The North American Reliability Corporation (NERC) recommends to shift all assessment areas from deterministic to probabilistic approaches [6, 7].

The NERC standards require an immediate response through automatic generation control in order to maintain frequency and tie line regulation, and a contingency reserve to restore the system to its pre-disturbance state within 15 minutes of a disturbance in order to prevent load curtailment [8]. The economic load dispatch of committed generating units can be generally be modified in the most economical way [9, 10] to maintain the operating risk within reasonable levels. It will not always be viable to maintain an acceptable risk as the operating penetration of intermittent energy sources increases. In such situations, ESS such as flywheel energy storage systems (FESS) can provide fast response to mitigate the operating risks.

A FESS can be used to store electrical energy in the form of kinetic energy, and can convert back to electrical energy when needed. Higher energy efficiency, larger instantaneous power, longer lifetime and environment friendly features are major advantages of FESS compared to other storage technologies [11-13]. Reference [14] provides comparative study of various ESS in power applications. An overview of FESS application in power systems is presented in [15], while [16] presents the control of high-speed FESS in space applications. A detailed report on design and loss analysis of high speed FESS is presented in [17, 18]. Most of these publications deal with

suitability of the FESS in different applications, design and loss analysis, but lack the direct-usability in quantitative risk assessment of power system operation. The reliability benefits of using an ESS in a wind-integrated power system is presented in [19]. The storage model used in [19] does not incorporate characteristics of any specific storage system, but rather uses an ideal model where the ESS is 'perfect' and can always deliver the power determined by its rating and its SOC. In contrast to past published literature, this paper proposes an integrated reliability model of FESS incorporating its inherent characteristics and component failures. The common practical topologies of FESS plants have been considered in the modelling. The impacts of variability of failure rates of the rotating parts has also been investigated in the paper.

2.3. Reliability Modelling of Flywheel Energy Storage System

A flywheel stores energy in the form of kinetic energy determined by the speed of its rotating mass. The SOC of a FESS is the amount of energy stored at a given time, and can be obtained using (2.1), where, I is the mass moment of inertia in kg-m^2, and $\omega(t)$ the rotational speed of the flywheel in rad/s at time t. At the maximum allowable rotational speed, the SOC is equal to its rated value, SOCrated.

$$\mathrm{SOC(t)} = \frac{1}{2} \mathrm{I} \times [\omega(\mathrm{t})]^2 \qquad (2.1)$$

A typical FESS consists of sub-systems grouped together to meet the required power and energy capacity [20, 21] as shown in Figure 2.1. Each sub-system contains transformer, switch gear, a cluster of flywheels, and a cluster controller. The cluster controller keeps track of the SOC and health of the associated flywheels and applies the operational logic to the cluster to carry out the required power exchange. A blowout of the components within each cluster of the sub-system are also shown in Figure 2.1. These consists of blocks of three major components, namely: flywheel energy storage unit (FESU), power control module (PCM) and a back to back converter. The back-to-back converter connected with FESU facilitates the power exchange between FESU and the grid.

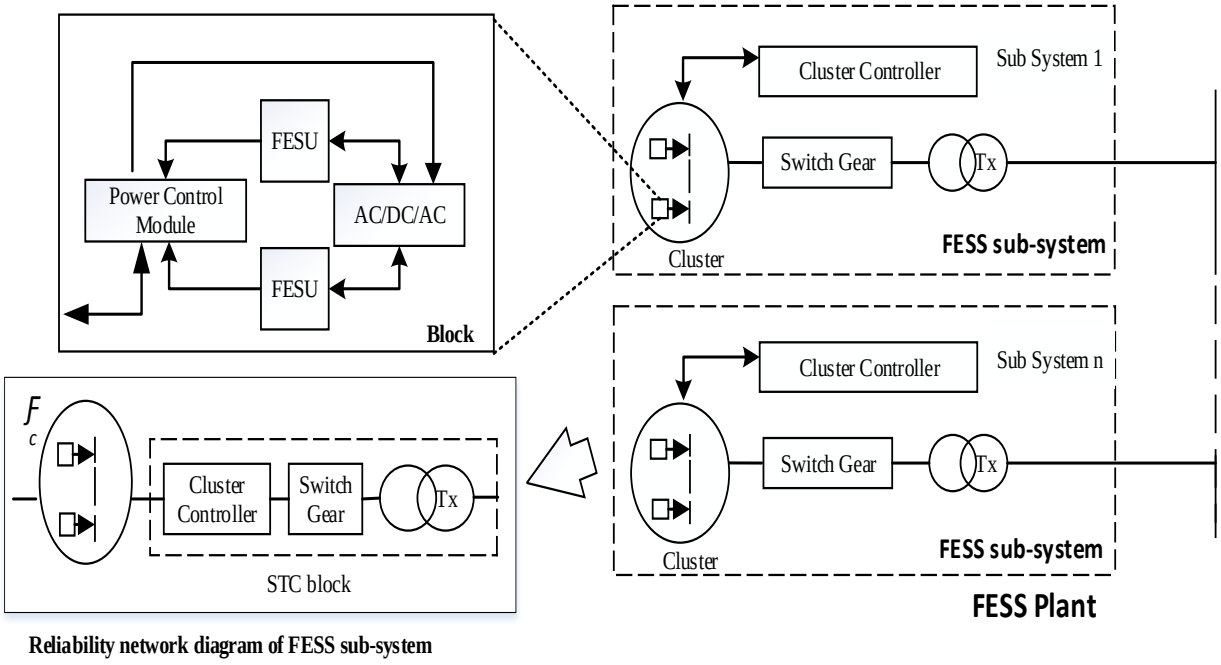

Figure 2. 1. Layout of a typical FESS plant, its sub-system, cluster components and reliability network diagram of the sub-system.

A cluster of flywheels can be represented by a discrete probability distribution of different SOC states, $\mathcal{F}^C(T)$ which the cluster may exhibit within a certain mission time, T as expressed in (2.2), where, S_i represents the ith SOC state, $P_i(T)$ the probability of the state within the mission time T, and $\sum_k P_k(T) = 1$. The last state in the distribution $\mathcal{F}^C(T)$ corresponds with the zero SOC of the cluster. Since each component inside the cluster can have two possible states, total number of states in $\mathcal{F}^C(T)$ equals to two raised to the power of total number of components. The total number states can be reduced by setting a criterion of removing the states with associated probabilities less than a set value.

$$\mathcal{F}^C(T) \sim \{(S_1, P_1(T)), (S_{k-1}, P_{k-1}(T)), \dots, (S_k, P_k(T))\} \tag{2.2}$$

Figure 2.1 also shows a reliability network diagram of the FESS sub-system. The combination of the switch gear, transformer Tx, and the cluster controller is referred to as STC block in this paper. All of these components are required to be functional for the block's successful operation. Assuming exponential times to failure [18] of the components, the equivalent failure rate λ_{eqv} of the STC block can be evaluated using (2.3). The probability of the STC block failing

in a mission time *T* given that it was operating successfully at the beginning of mission is known as its outage replacement rate (ORR) [16], and can be obtained using (2.4) for a mission time *T*.

$$\lambda_{eqv} = \sum_i \lambda_i \tag{2.3}$$

$$\mathrm{ORR_{eqv}(T)} = 1\text{-}e^{-(\lambda_{eqv})T} \tag{2.4}$$

The 2-state Markov model of the STC block is convolved with the discrete distribution $\mathcal{F}^C(T)$ to obtain an overall SOC probability distribution of each sub-system, $\mathcal{F}^S(T)$ as expressed in (2.5). In the similar manner, the probability distribution of SOCs for overall plant can be created by convolving the probability distributions associated with each sub-system constituting the plant.

$$\mathcal{F}^S(T) \sim \left\{ \begin{array}{c} \left(S_1, P_1(T) * \left(1 - ORR_{eqv}(\mathrm{T})\right)\right), .. \\ \ldots, \left(S_{k-1}, P_{k-1}(T) * \left(1 - ORR_{eqv}(\mathrm{T})\right)\right), \ldots \\ \ldots, \left(S_k, P_k(T) * \left(1 - ORR_{eqv}(\mathrm{T})\right) + ORR_{eqv}(\mathrm{T})\right) \end{array} \right\} \tag{2.5}$$

The components inside a cluster shown in the blowout-view of Figure 2.1 are each represented by a two-state model, using the ORR of the respective components for mission time of interest. The FESU can be represented by a reliability network model consisting of a simple series configuration of its major components that are required to be functional for the unit's successful operation, as shown in Figure 2.2.

The equivalent failure rate and hence the equivalent ORR of each FESU can be obtained from the reliability network in Figure 2.2 using (2.3) and (2.4). The reliability model of the each block in the cluster can be obtained using a reduced event tree diagram [22] which is also shown in Figure 2.2. Each branch in the event tree corresponds to the occurrence of a particular event in the mission time. The bar sign above a component represents its failure during the mission. The probability associated with each event can be obtained using the ORR of the associated components for the given mission time. The tree diagram is used to obtain the discrete probability distribution of a cluster SOC depending on the number of FESU in the cluster. Figure 2.2 shows an example topology with 2 FESU sharing a PCM, and resulting in three discrete states of 100%, 50% and zero SOC. Alternate topologies may have each FESU with its own PCM, or multiple FESU with a single PCM and converter, and the different cluster topologies can easily be accommodated in the proposed framework. The choice can influence the reliability and the

economics associated with the topology. The "top-down" modelling approach presented in this paper extends down to modular blocks and components and is flexible to integrate the models in a "bottom-up" evaluation to obtain the SOC model of the overall FESS.

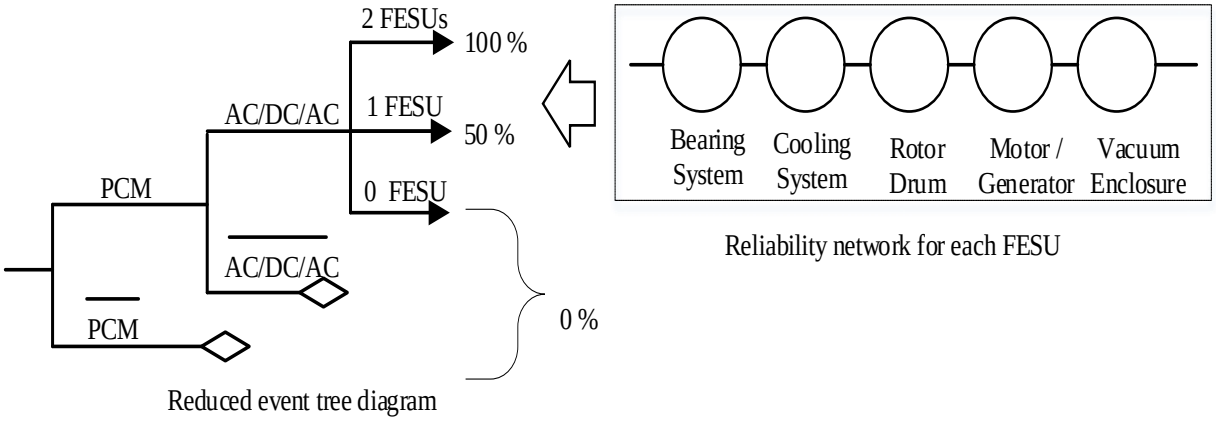

Figure 2. 2. Cluster SOC model using a reduced event tree diagram, and reliability network of FESU.

The SOC of a FESU changes continuously during system operation due to charging and discharging. The change in SOC after a Δt duration can be evaluated using (2.6).

$$SOC(t+\Delta t)=SOC(t)+\gamma \times P(t) \times \Delta t - \int_{t}^{t+\Delta t} P_{loss}(t)\, dt \quad (2.6)$$

Where, P_{loss} is the power loss in the flywheel which depends on its rotational speed, P(t) is the power available to charge or discharge, and $\gamma = \{1, -1, 0\}$ for charging, discharging and stand-by operation respectively during the interval Δt. A detailed study of the estimation of different types of losses in FESU is discussed in [17]. The charging power $P(t) \leq P_{max}^{Chrg}$ and $P(t) \leq P_{max}^{Dischrg}$ respectively for charging and discharging operation. The maximum charging P_{max}^{Chrg} is limited by the FESU motor rating, and the maximum discharging power $P_{max}^{Dischrg}$ is given by (7) where SOC(t) is the initial FESU SOC at the beginning of the Δt duration.

$$P_{max}^{Dischrg}=\min\left\{P_{rated}, \frac{SOC(t)-SOC_{min}+Loss}{\Delta t}\right\} \quad (2.7)$$

A FESS connected to a power system can absorb or mitigate the disturbances. The assisting capacity C of the FESS available to mitigate a disturbance of magnitude X can be obtained from the SOC model and is expressed in (2.8). A negative X indicates excess generation, and calls for

a charging operation of the FESS, and vice-versa. The residual disturbance X' after mitigation can be obtained using (2.9)

$$C = \begin{cases} -\min(P_{max}^{Dischrg},\ |X|; if\ X > 0 \\ \min(P_{max}^{Chrg},\ |X|; if\ X < 0 \\ 0; Otherwise \end{cases} \quad (2.8)$$

$$X' = X + C \quad (2.9)$$

2.4. Application of the Proposed Model and Analysis

The application of the presented reliability framework to assess the SOC model of a FESS is illustrated on a test power system integrated with a FESS constituting 60 clusters of 10 FESU each with power and energy ratings of 0.5 MW and 100 kWh, respectively. The ORR of each FESS component was evaluated using (2.3) and (2.4) with reference to failure rate data provided in [19] and [12]. Figure 2.3 shows the SOC model of the FESS plant for a range of mission times, given that each FESU (Topology I) is initially at 20% SOC and the components are fully functional at the start of the mission. Figure 2.3 shows that the SOC distribution changes with an increase in mission time, with most probable SOC state shifting from large capacity to a smaller one. Figure 2.4 shows the SOC models for two cluster topologies. Topology I has two FESUs sharing a PCM and a converter, and Topology II has a PCM and a converter for each FESU. The SOC distributions of the two topologies are almost identical for the two operating mission times considered in the study. The difference in reliability of the two topologies are mainly contributed by the PCM and converter failure rates. These are relatively low for electronic components, and since the small mission times result in small ORR of these components, the difference in the network configuration does not reflect much in terms of SOC distribution. This suggest that the topology of the plant does not significantly affect the SOC model in operating risk evaluation, and choice of configuration aligns more with system economics.

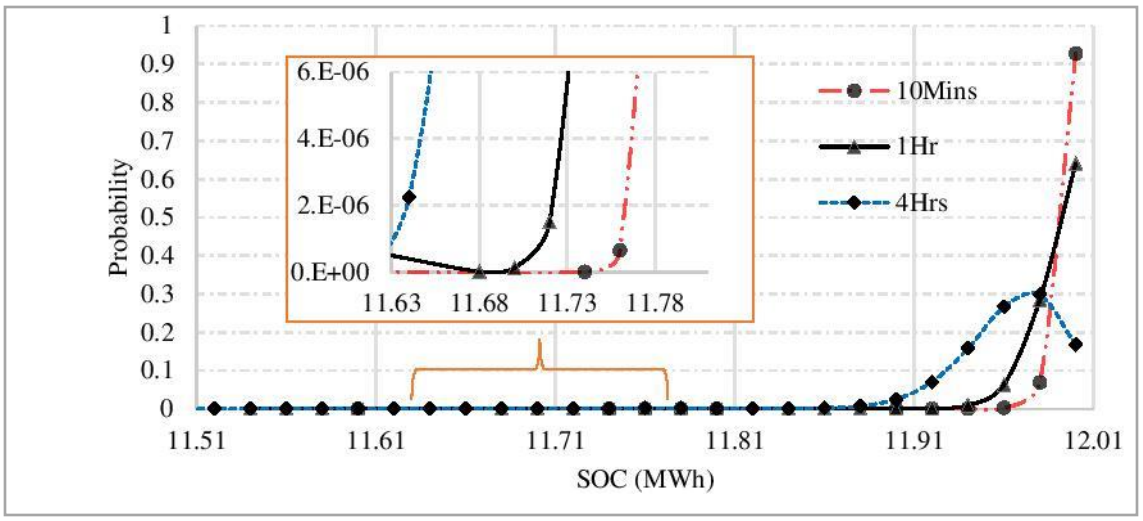

Figure 2. 3. Discrete SOC distribution for various mission times with 20% initial SOC of FESS considering Topology I.

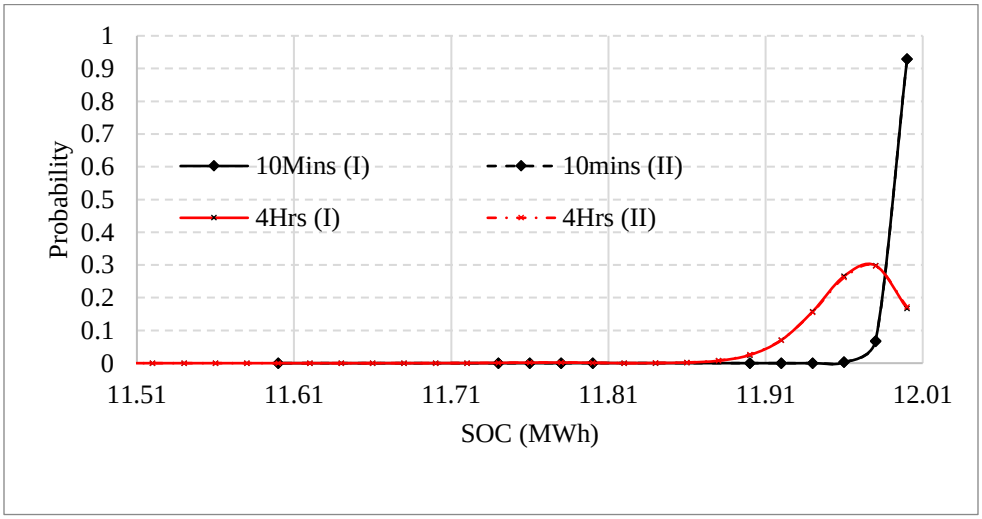

Figure 2. 4. Discrete SOC distribution for various mission times with 20% initial SOC of FESS considering Topology I and II.

The flywheel rotor at very high speeds can be exposed to high failure rates. A study was carried out to assess the impact of rotor failure rate on the SOC distribution, assuming that the failure rate is increased by a multiple of 'K' when the SOC exceeds 50%. Figures 2.5 and 2.6 show the SOC distribution for mission times of 10 minutes and 4 hours respectively, considering 60% initial SOC with different 'K' values. The SOC distribution shift to the right, and the probability associated with highest SOC state decreases as K is increased. The change in SOC distribution is more pronounced as the mission time in increased. This implies that for shorter operating times,

such as in power system risk assessment in the operating domain, the assumption of a constant failure rate of the rotating drum irrespective of SOC of the associated flywheel is reasonably acceptable, while in case of longer mission times, the implications of having higher failure rate of rotating parts at higher speed of flywheel will be more pronounced.

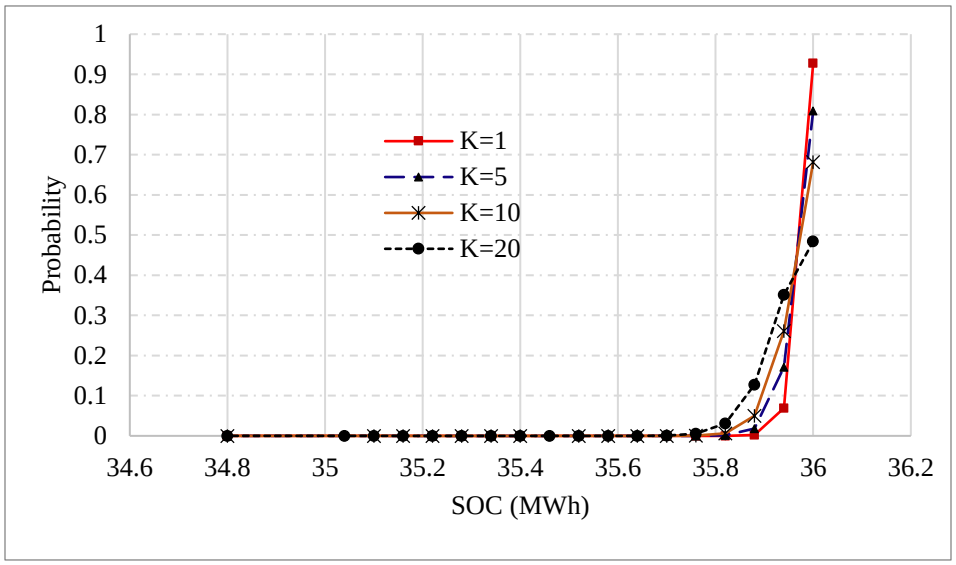

Figure 2. 5. Discrete SOC distribution with varying failure rates of the rotor drum for 10-minutes mission time.

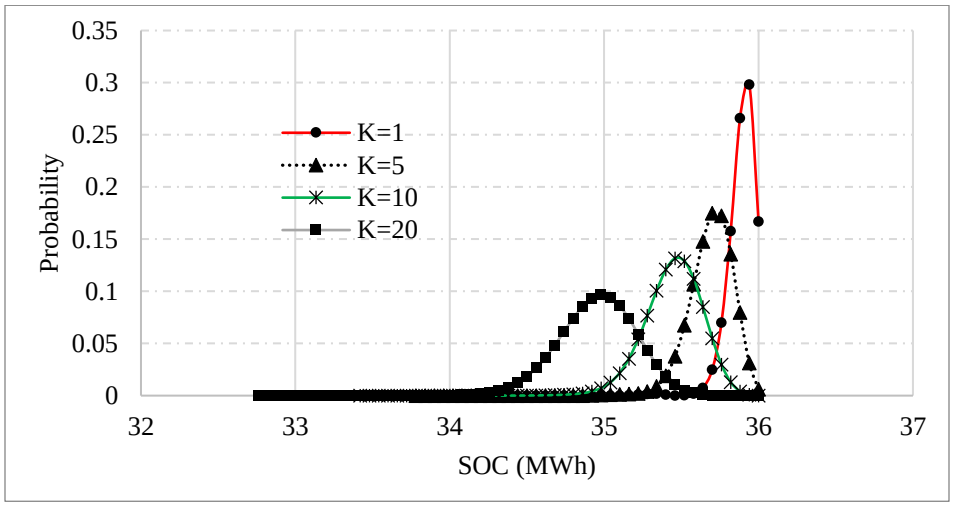

Figure 2. 6. Discrete SOC distribution with varying failure rates of the rotor drum for 4-hours mission time.

A study was done to demonstrate the application of the probabilistic FESS model in mitigating power disturbance during power system operation. A probability distribution of disturbance can be created using probabilistic wind power model and load forecasting error models. Figure 2.7 shows a hypothetical disturbance model to which a Topology I FESS plant was employed to respond within a mission time of 10 minutes. The convolution of the SOC model and the disturbance model based on (2.8) and (2.9) gives the new probability distribution of the disturbance after mitigation by FESS, as shown in Figure 2.8. It shows that the disturbance distribution shifts toward the "zero" disturbance axis with the increase in the initial SOC. Figure 2.8 shows that the original expected disturbance of 90.3 MW is mitigated to 22.5, 12.0, 6.2, and 1.8 MW respectively as the initial SOC is increased from 20% to 40%. This is because a high initial SOC in the FESS at the time of major contingency helps the FESS to absorb the disturbances more effectively and improves the ability of the operating system to withstand disturbances, but at the same time, it also limits the FESS's ability to capture surplus energy in a system with large wind penetration. The disturbance model considered in the study together with probabilistic model of FESS can be used to quantify the reliability benefits of FESS in power system operation.

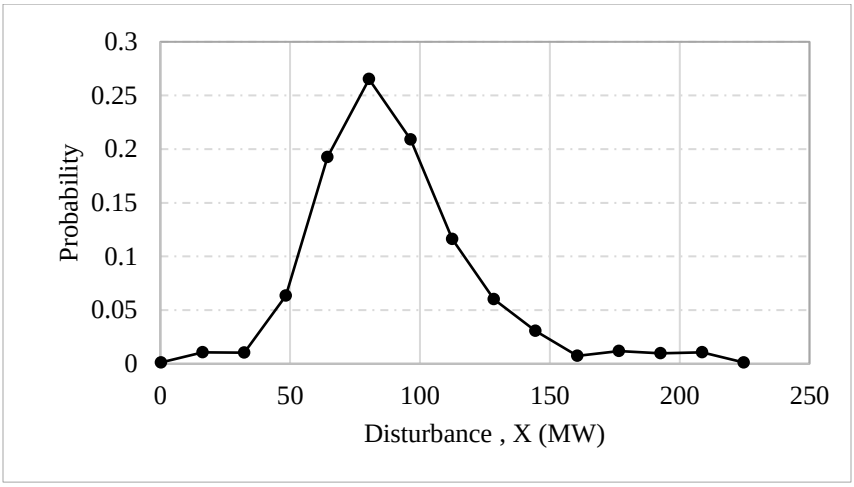

Figure 2. 7. Hypothetical wind/load disturbance model.

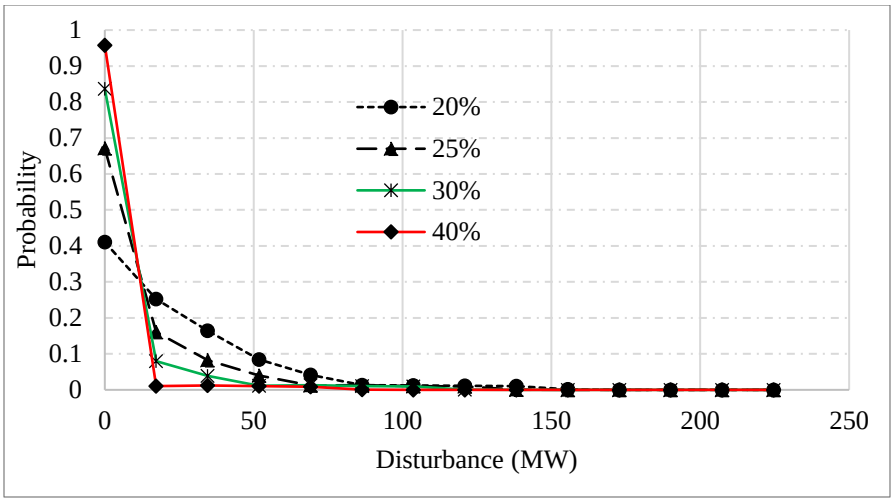

Figure 2. 8. New disturbance after mitigation by FESS with various initial-SOC levels.

2.5. Conclusion

This paper presents a reliability model of FESS incorporating its operational modes, the failure mechanism of its major components and their interoperability for acceptable performance in a power system. The reliability model is embedded in the proposed methodology to obtain the FESS model in the form of a discrete SOC distribution, which depends on the initial conditions and the length of the mission times. The FESS model can be convolved with system disturbance models to quantify the contribution of FESS in mitigating power system operating risks. The operating mission time is dictated by the market in which the FESS participates and the corresponding domain of study. The SOC distribution is significantly influenced by the mission duration. The capacity of the most probable state and the expected SOC value decreases as the mission time is increased. The initial SOC of the FESS plant at the time of disturbance dictates its ability to respond effectively to the system disturbances. A high initial SOC of FESS at the time of disturbance mitigates the disturbance more effectively, but at the expense of its ability to store the surplus energy in the system. High speed rotating parts are generally exposed to higher failure rates than electronic components of a system. The failure rates of FESU rotor drum at high SOC speeds can be much higher than that at low speeds. Although these impacts are notable at long mission times, they are insignificant at acceptable capacity response times in power system operation. FESS are available in different plant topologies, and they mainly vary in the usage of

additional power electronics components. The different topologies however have little impact on the FESS model for the operating times considered since the failure rates of the electronic components are relatively small. The choice of plant topology is determined by the system economics. The simplicity and usability of the proposed model in probabilistic risk assessment of power system operation is justified by its application in disturbance mitigation as presented in the paper.

2.6. References

[1] P. Hu, "Reliability evaluation of generating systems containing wind power and energy storage", *IET Generation, Transmission and Distribution*, vol. 3, pp. 783–791(8), August 2009.

[2] Global Wind Energy Council, "Global wind report annual market update 2015", Wind energy Technol., pp. 1–76, 2015.

[3] S. Ghosh and S. Kamalasadan, "An energy function-based optimal control strategy for output stabilization of integrated DFIG-flywheel energy storage system", *IEEE Transactions on Smart Grid*, vol. 8, no. 4, pp. 1922–1931, 2017.

[4] N. S. Hasan, M. Y. Hassan, M. S. Majid and H. A. Rahman, "Review of storage schemes for wind energy systems," *Renewable and Sustainable Energy Reviews*, vol. 21, no. Supplement C, pp. 237 – 247, 2013.

[5] G. O. Suvire and P. E. Mercado, "Active power control of a flywheel energy storage system for wind energy applications", *IET Renewable Power Generation*, vol. 6, no. 1, pp. 9-16, January 2012.

[6] N. Abdel-Karim, D. Calderon, T. Coleman, and J. Moura, "A hybrid probabilistic assessment using different renewable penetration scenarios in the North American bulk power system", Probabilistic Methods Applied to Power Systems (PMAPS), *2016 International Conference on. IEEE*, 2016, pp. 1–5.

[7] NERC, "NERC 2014 probabilistic assessment report", NERC, Tech. Rep., April 2014.

[8] N. A. E. R. Corporation, "Reliability standards for the bulk electric systems of north America", NERC, Atlanta, GA, Tech. Rep., 2013.

[9] M. Fotuhi-Firuzabad, R. Billinton, and S. Aboreshaid, "Spinning reserve allocation using response health analysis", *IEE Proceedings-Generation, Transmission and Distribution*, vol. 143, no. 4, pp. 337–343, 1996.

[10] R. Karki, S. Thapa, and R. Billinton, "Operating risk analysis of wind-integrated power systems", *Electr. Power Components Syst.*, vol. 40, no. 4, pp. 399–413, 2012.

[11] X. Zhang and J. Yang, "A DC-link voltage fast control strategy for high-speed PMSM/G in flywheel energy storage system", *IEEE Transactions on Industry Applications*, vol. PP, no. 99, pp. 1-1.

[12] R. Hebner, J. Beno, and A. Walls, "Flywheel batteries come around again", *IEEE spectrum*, vol. 39, no. 4, pp. 46–51, 2002.

[13] S. Vazquez, S. M. Lukic, E. Galvan, L. G. Franquelo and J. M. Carrasco, "Energy storage systems for transport and grid applications", *IEEE Transactions on Industrial Electronics*, vol. 57, no. 12, pp. 3881–3895, 2010.

[14] M. Farhadi and O. Mohammed, "Energy storage technologies for high-power applications", *IEEE Transactions on Industry Applications*, vol. 52, no. 3, pp. 1953-1961, May-June 2016.

[15] M. I. Daoud, A. S. Abdel-Khalik, A. Massoud, S. Ahmed and N. H. Abbasy, "On the development of flywheel storage systems for power system applications: A survey", *2012 XXth International Conference on Electrical Machines*, Marseille, 2012, pp. 2119-2125.

[16] B. H. Kenny, P. E. Kascak, R. Jansen, T. Dever and W. Santiago, "Control of a high-speed flywheel system for energy storage in space applications", *IEEE Transactions on Industry Applications*, vol. 41, no. 4, pp. 1029-1038, July-Aug. 2005.

[17] F. Deiana, A. Serpi, J. Abrahamsson, I. Marongiu and G. Gatto, "Extensive losses estimation of a novel high-speed permanent magnet synchronous machine for flywheel energy storage systems", *2016 XXII International Conference on Electrical Machines (ICEM)*, Lausanne, 2016, pp. 1728-1734.

[18] C. Zhang, K. J. Tseng, T. D. Nguyen and S. Zhang, "Design and loss analysis of a high speed flywheel energy storage system based on axial-flux flywheel-rotor electric machines", *2010 Conference Proceedings IPEC*, Singapore, 2010, pp. 886-891.

[19] S. Thapa and R. Karki, "Reliability benefit of energy storage in wind integrated power system operation", *IET Generation, Transmission & Distribution*, vol. 10, no. 3, pp. 807–814, 2016

[20] [http://temporalpower.com/wp-content/uploads/2014/06/Features-and-Benefits-of-the-Temporal-Flywheel-Energy-Storage-System1.pdf, accessed: 9/2016]

[21] [http://beaconpower.com/wp content/themes/beaconpower/inc/beacon_power_brochure_081414.pdf. accessed 9/2016]

[22] R. Bilinton and R. Alan, *Reliability Evaluation of Engineering Systems*. New York: Plenum, 1996.

PREFACE TO CHAPTER 3: INTEGRATED DISTURBANCE RESPONSE MODELLING TO QUANTIFY THE OPERATIONAL RELIABILITY BENEFITS OF FLYWHEEL ENERGY STORAGE SYSTEMS

Chapter 3 is organized as manuscript and is thus essentially a self-contained chapter. The manuscript is submitted to *IEEE Transactions on Sustainable Energy* and is currently under second round of review. A novel framework for generation response risk evaluation of wind-integrated power system incorporating various disturbances that may arise during the system operation is presented in this chapter. The application of proposed methodology builds on the reliability modelling of flywheel energy storage system (FESS) developed in previous chapter and introduces a new-relative risk index to assess the impacts of increasing operating wind penetration and quantifies the reliability benefits of FESS. The chapter shares a modicum of literatures and descriptions on FESS modelling with Chapter 2. Second and third specific objectives of the research as stated in Section 1.5 are addressed in this chapter.

CHAPTER 3: INTEGRATED DISTURBANCE RESPONSE MODELLING TO QUANTIFY THE OPERATIONAL RELIABILITY BENEFITS OF FLYWHEEL ENERGY STORAGE SYSTEMS

Saket Adhikari, Rajesh Karki, *Senior Member, IEEE*

3.1. Abstract

Growth of renewable power penetration has exposed modern power systems to high operating risks, due to intermittency and uncertainty inherent in such energy sources. It is therefore essential to assess the associated risks and explore potential resources to mitigate these risks. This paper presents an integrated reliability model of a flywheel energy storage system (FESS) incorporating its specific charge/discharge, storage, performance and failure characteristics. A novel approach in evaluating the response risk to system disturbances is proposed. Additionally, a new comparative risk index designated as the Response Risk Multiplication Factor has also been proposed to quantify the impact of operating wind penetration in system operation and the effectiveness of resources with high ramp rates in providing controllability to highly intermittent energy sources like wind power. A disturbance uncertainty model incorporating wind power and FESS based on time-dependent conditional probability approach is created. The model embeds posterior probability approach to utilize the known information on time of day and FESS SOC. The developed model is applied to the IEEE Reliability Test System to illustrate its usability in assessment of the impact on power system operating risk due to large operating penetration of wind power and effectiveness of FESS in risk mitigation.

3.2. Introduction

Electricity generation using renewable sources is rapidly growing with increasing environmental concerns regarding fossil fuels. The growth in renewable energy usage occurred in

the past decade clearly portrays a promising future of renewable energy. Many countries have implemented policies such as the Renewable Portfolio Standard (RPS), to promote renewable energy. RPS is a commitment to produce a certain fraction of total generation using renewables within a specified time-frame [1]. The total global wind power production at the end of 2016 was 486.8 GW, with cumulative market growth of 12% and GWEC forecasts that the cumulative installed capacity will increase to over 800 GW by the end of 2021 [2]. It is apparent that wind power is the most preferred renewable energy source (RES) for bulk power production and is likely to be a mainstream source of energy in the near future. Intermittency and uncertainty inherent in wind power pose significant threat to power system reliability during operation, especially if the operating wind penetration shares a significant portion of the load [3-5]. Increasing dominance of wind power in generation mix calls for probabilistic methods for assessing the resources availability and their impact on power system operation [6]. A time-dependent probabilistic wind power model suitable for capturing the wind-speed profile that a typical wind site may exhibit during different times of day is presented in this paper. The proposed model can be easily incorporated in probabilistic operational risk assessment of a power system.

In power system operation, the committed generating units are normally dispatched to minimize the system operating costs, and the method is known as the economic load dispatch (ELD). This practice together with deterministic methods of allocating operating reserve, however, does not ensure adequate response from the operating reserve capacity within the margin time following a major disturbance. As a result, ELD may lead to unacceptable operating reliability, since economics and reliability often compete with each other. The system's ability to provide adequate response capacity is further limited by high penetration of RES into the system. Highly intermittent energy sources such as wind have thus created challenges in maintaining system reliability in power system operation. With rapid increase in RES penetration in power systems throughout the world, system operators are becoming increasingly concerned with their impacts on reliable and economic system operation. The ability to quantify the operational risks associated with probable contingencies of different magnitudes for given operating scenario will help planners and operators to make an informed decision. Probabilistic risk assessment thus becomes inevitable in wind-integrated power system planning and operation. The North American Reliability Corporation (NERC), therefore, recommends to shift all assessment areas from deterministic to probabilistic approaches [6, 7].

Response Risk (RR) is defined as the probability that the response capacity available within a margin time, following a disturbance, will be less than the required capacity [8]. The NERC standards require that an immediate response should be available through automatic generation control (AGC) in order to maintain frequency and tie line regulation and the contingency reserve should be able to restore the system to its pre-disturbance state within 15 minutes of a disturbance in order to prevent load curtailment [9].

The response risk evaluation approach proposed in [10] includes the effect of the response rate of the responding unit and the probability that the responding unit fails during the response period. A major limitation of this approach is that it assumes only the units operating with spinning reserves and responsible for providing the response to a disturbance are exposed to failure during the response period. But in fact, even the operating units that are fully loaded and/or cannot participate in capacity response are likely to fail during the response period thereby creating another disturbance in the supply-demand balance. References [11] and [12] slightly modify the response risk evaluation approach by introducing a new security constraint that the available response capacity of the committed units within a certain margin time be greater than the required regulating margin. The required regulating margin as defined in the literature is a fixed percentage of spinning reserve. Reference [12] extends the same idea to include the wind power in the evaluation framework. This hybrid approach of combining probabilistic evaluation framework with a deterministic constraint of a constant regulating margin does not focus on the magnitude of the major disturbance toward which the system is responding. But rather, the approach tries to focus on probability of maintaining a pre-defined amount of regulating margin. And especially, with large amount of wind energy being injected into the system, the approach calls for large amount of regulating capacity from conventional units. Moreover, the reported method to modify ELD in the most economical way to keep the operating risk within acceptable value will not always be a viable option as operating penetration of wind power in the system increases. The need for resources with fast ramp rate thus becomes inevitable. It is therefore very essential to have the ability to make quantitative assessment of associated risks in system operation, and to investigate the full potential of suitable resources such as energy storage systems in order to mitigate these risks. These limitations in the reported literature are addressed in the new approach proposed in this paper. The consideration of active capacities of all remaining healthy units in creating the capacity response model, regardless of their individual share in the reserve margin, addresses the

possible additional disturbances from the loss of any remaining healthy unit(s) during the response time and is an important consideration in response risk evaluation from practical operational point of view. Instead of focusing on the probability of maintaining a pre-defined amount of regulating margin during system operation, the evaluation of the probability of adequate and timely response toward a major contingency disturbance, as proposed in this paper, gives a more realistic appraisal of the response risk in the system operation and insights for the system operators to avert or minimize the impact of identified major contingencies.

Among the host of past literatures [10-17] on power system security, a few are focused on generation response risk evaluation with very limited work on incorporating energy storage system (ESS) in the evaluation framework. Reliability benefits of ESS in power system operating risk is presented in [13]. However, the risk assessment is limited to unit commitment risk (UCR) which does not consider the characteristics of disturbances and associated responses, or the ramping abilities of the committed units. Furthermore, the storage model used in the literature does not incorporate characteristics of any specific storage system. But rather, uses an ideal model where storage system is 'perfect' and can always deliver the power determined by its power rating and state of charge (SOC). Reference [16] presents a simulation-based approach for operational adequacy analysis of wind-integrated power system and sums up the operational risk in terms of expected energy not served (EENS) in the time horizon of months. Reference [17] presents a more general framework to perform the similar task as in [16] and evaluates the operational risk in terms of UCR and EENS. Although the approaches presented in [16] and [17] provide an important insight of comparatively long-term operational risk profile to the system planners, it has limited significance in terms of analysis of the generation response to the major contingency disturbances within a short operational time frame. These limitations are addressed in this paper through a new response risk evaluation framework that is particularly focused on the system's generation response capacity to respond to the specific major disturbances.

A flywheel energy storage system (FESS) can be used to store electrical energy in the form of rotational energy, and can convert the stored energy back into electrical energy. Higher energy efficiency, larger instantaneous power, longer lifetime and environment friendly features are major advantages of FESS compared to other storage technologies [20-22]. An overview of power system applications of FESS is presented in [21], while [22] and [23] deal with design and loss analysis of FESS. Majority of the published literature deal with investing and analyzing the

suitability of the FESS in different applications, design and loss analysis, but lack the direct-usability in quantitative risk assessment of power system operation. This paper provides a new contribution by developing an integrated mission-oriented reliability model of FESS incorporating its inherent charge / discharge characteristics and component failures.

This paper presents a time dependent disturbance model that recognizes random short-term deviation from a given initial system operating state due to random forced outages of committed generating units, uncertainty in wind power fluctuation and load variation. Unlike widely reported short-term wind power models [12, 16] the proposed disturbance model incorporates rising and falling diurnal trends in modeling wind power uncertainty. Identifying positive and negative magnitudes of power disturbances are particularly important in embedding the disturbance model with FESS charging and discharging characteristics, and this feature of the proposed model is a new contribution that enables the assessment of response risk mitigation by ESS. The integration of the uncertainties associated with different operating variables, mainly the wind speed, load variation and forced outages of committed units in creating the disturbance model, and the combination of the integrated disturbance model with the proposed FESS response model to quantify the impact of ESS on operating risk mitigation are the key contributions of this paper.

An index designated as response risk multiplication factor (RRMF) is introduced that measures the relative change in the response risk (RR) due to addition of wind energy into the system. The index can be used to quantify the impact of increasing operating wind penetration on the system RR. The RRMF is also used to measure the relative change in RR due to combined effect of wind and ESS. In this case, the index serves to quantify the benefits of FESS in mitigating the system RR to maintain operational reliability.

3.3. Reliability Modelling of Flywheel Energy Storage System

A flywheel stores energy in the form of mechanical energy determined by the speed of its rotating mass. The SOC of a FESS is the amount of energy stored at a given time, and can be obtained using (3.1).

$$SOC(t) = \frac{1}{2} I\omega(t)^2 \tag{3.1}$$

Where, I is the moment of inertia, and ω the rotational speed of the flywheel at time t. At the maximum allowable rotational speed, the SOC is maximum or equal to its rated value, SOC_{rated}.

Figure 3.1 shows the major components that constitute a typical Flywheel Energy Storage Unit (FESU). A magnetic bearing system and a vacuum enclosure provides a near-frictionless environment for the rotor's rotation. A permanent magnet synchronous machine operates in both motor and generator modes. The machine is enclosed inside a vacuum chamber, and a dedicated cooling system is provided to dissipate the heat generated. A back-to-back converter connected with each FESU facilitates the power exchange between FESU and the grid. A power control module (PCM) keeps track of the SOC and state of health of the associated FESU. Figure 3.2 shows a cluster of FESUs. A typical FESS plant will have multiple clusters grouped together to meet the required power and energy capacity. A cluster controller is provided to each cluster, which keeps track of the SOC and applies the operational logic to the cluster to carry out power exchange.

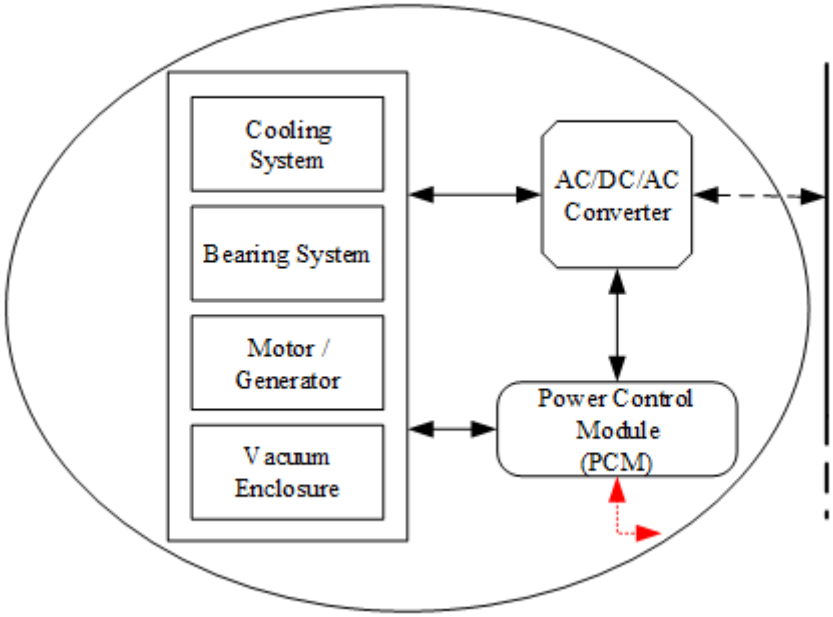

Figure 3. 1. Flywheel energy storage unit (FESU).

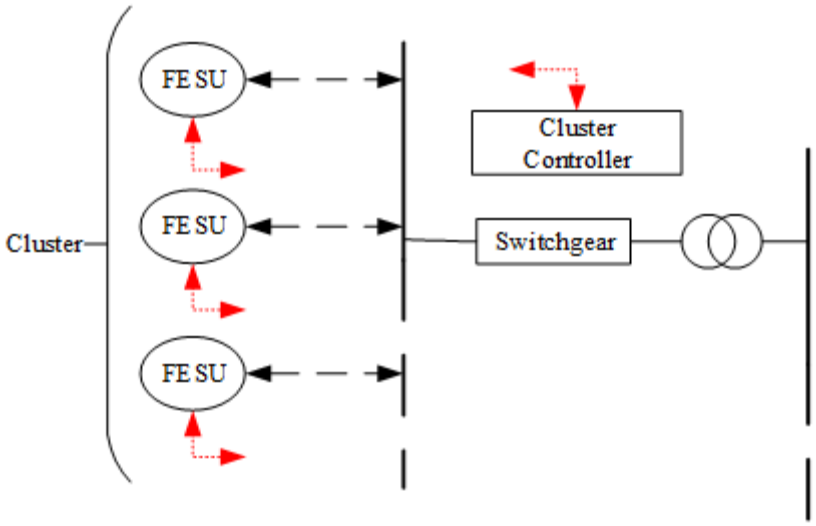

Figure 3. 2. Cluster of FESUs.

The SOC of a flywheel changes continuously in time due to charging, discharging and stand-by operation. The new SOC after a Δt duration can be evaluated using (3.2).

$$SOC(t+\Delta t)=SOC(t)+y \times P(t) \times \Delta t - \int_{t}^{t+\Delta t} P_{loss}\, dt \quad (3.2)$$

Where, P_{loss} is the power loss in the flywheel, $P(t)$ is the power available to charge or discharge, and y = {1, -1, 0} for charging, discharging and stand-by operation respectively during the interval Δt. P_{loss} is a function of rotational speed of the flywheel. A detailed study in estimation of different types of losses in FESU is presented in [22] and [22]. For charging operation, $P(t) \leq P_{max}^{Chrg}$, and for discharging operation, $P(t) \leq P_{max}^{Dischrg}$. P_{max}^{Chrg} is maximum charging power limited to power rating of the generator, while the maximum discharging power, $P_{max}^{Dischrg}$ is given by (3.3).

$$P_{max}^{Dischrg}=\min\left\{P_{rated}, \frac{SOC(t)-SOC_{min}+Loss}{\Delta t}\right\} \quad (3.3)$$

The FESU can be represented by a reliability network model consisting a series configuration of its major components that are required to be functional for the unit's successful operation. Assuming exponential times to failure [24] of the major components, the equivalent failure rate of a FESU can be evaluated using (3.4)

$$\lambda_{eqv} = \sum_{n\in\varphi_{CF}} \lambda_n \quad (3.4)$$

Where, λ_n is the failure rate of n^{th} component from φ_{CF}: set of all critical components of FESU.

The probability of a FESU failing in a mission time given that it was operating successfully at the beginning of mission is known as its outage replacement rate (ORR) [10]. The ORR is time dependent and can be obtained using (3.5) for a mission time T.

$$ORR(T)=1-e^{-(\lambda_{eqv})T} \quad (3.5)$$

By obtaining the ORR of a FESU using (3.4) and (3.5) for a given mission time, the SOC of a FESS can be modeled as a discrete probability distribution with posterior probability conditional upon the known initial conditions of its SOC and system components' status.

An example is illustrated considering a FESS constituting 60 clusters of 10 FESUs each with power rating (P_{rated}) and energy rating (SOC_{rated}) of 0.5 MW and 100 kWh respectively. The ORR for a mission time of 10 minute were evaluated using (3.4) and (3.5), based on the failure rate data provided in [25] and [26]. Table 3.1 shows the SOC model for a 10 minute mission time conditional upon the initial SOC of each of FESUs being 50% of SOC_{rated} and the components being fully functional at the start of the mission.

Table 3. 1. SOC model of FESS plant.

State #	SOC (MWh)	Probability
1	30	0.960588
2	29.95	0.038383
3	29.9	0.000765
4	29.85	1.02E-05
5	29.5	0.000244
-	-	-
-	-	-
-	-	-
28	0	2.093E-07

3.4. Short Term Wind Power Modelling

Wind speed variation within a day follows a diurnal pattern of rising, flat or falling wind trend periods. This short-term characteristics of wind is illustrated using wind speed data obtained from the National Renewable Energy Laboratory (NREL) [27] collected at 10 minute time intervals for a site in North Dakota over a period of three years. Figure 3.3 shows the plot of average wind speeds for the 10 minutes interval for a total of 144 intervals or 24 hours within a particular day. The wind profile between 3 AM and 9 AM and between 11 AM to 4 PM show falling trends in the wind speed, where the falling slope is sharper in the afternoon. Similarly, wind speed profile has rising trend from 4 PM to 12 AM.

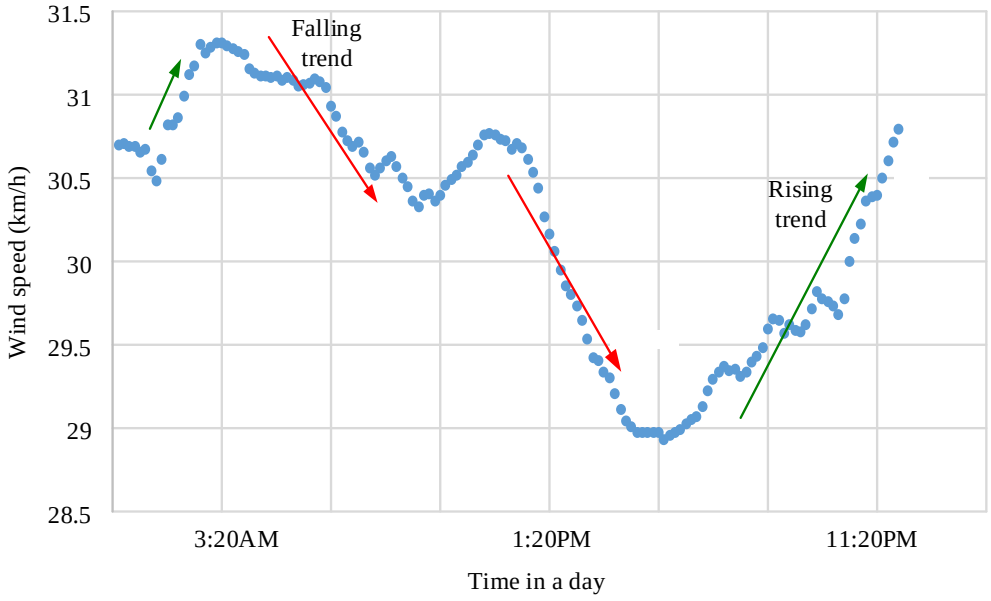

Figure 3. 3. Average wind speed profile in a day.

A conditional probability approach is used to obtain a short-term wind speed model following a major contingency disturbance conditional upon the known conditions prior to the disturbance. The known wind conditions are the initial wind speed (IWS) at the time T when the contingency just occurred, and the time of day of such occurrence lying in the rising, falling or flat trend of the historical wind profile. A set S of wind speed data in (3.6) can be obtained either from historical wind speed data x, or from a series of synthetic data from a statistical model, such as ARMA [28], in the absence of adequate historical data.

$$\mathcal{S} = \{x_{T+\Delta T} : x_T = IWS, x_T \subset \mathcal{R}\} \quad (3.6)$$

Where ΔT is the wind speed data interval which is equal or less than the margin time, and $\mathcal{R}$ is a set of wind speed data in the rising, falling or flat wind profile trend in which the IWP lies. Based on Sturges' rule [29], the number ($\mathcal{N}_b$) and width ($\mathcal{W}$) of class intervals and can be found using (3.7) and (3.8) respectively.

$$\mathcal{N}_b = 1 + 3.3 \text{ x} \log|\mathcal{S}| \tag{3.7}$$

$$\mathcal{W} = \frac{\text{Max}\{\mathcal{S}\} - \text{Min}\{\mathcal{S}\}}{|\mathcal{N}_b|} \tag{3.8}$$

The data in set $\mathcal{S}$ is divided into subsets, where subset $\mathcal{S}_i$ falling in the ith interval is given by (9). $\mathcal{B}_i^{min}$ and $\mathcal{B}_i^{max}$ shown in (3.10) and (3.11) respectively represent the lower and the upper limit of the i^{th} interval The mid-point B_i represents the wind speed for the interval i. A discrete probability distribution of wind speed within the margin time, conditional upon given IWS at time T is created, where the probability of the wind speed Bi is obtained using (3.12). This wind speed model is designated as the conditional wind speed distribution (CWSD).

$$\mathcal{S}_i = \left\{x_{T+\Delta T} : \mathcal{B}_i^{\min} \leq x_{T+\Delta T} < \mathcal{B}_i^{max}\right\};\ \mathcal{S}_i \subset \mathcal{S}, \forall\, i \leq \mathcal{N}_b \tag{3.9}$$

$$\mathcal{B}_i^{min} = \text{Min}\{\mathcal{S}\} + \mathcal{W} \text{ x } (i-1) \tag{3.10}$$

$$\mathcal{B}_i^{max} = \text{Max}\{\mathcal{S}\} - \mathcal{W} \text{ x } (i-1) \tag{3.11}$$

$$\text{P}\left(\overline{B_i}\right) = \frac{|\mathcal{S}_i|}{|\mathcal{S}|} \tag{3.12}$$

The CWSD can be transformed into conditional wind power distribution (CWPD) using Wind Turbine Generator (WTG) power curve characteristics [30].

3.5. Integrated Disturbance Modelling

This paper focuses on the operating reliability that is quantified by the ability of the system to respond adequately to major disturbances. This section presents the development of an integrated disturbance uncertainty model based on time-dependent and posterior probability approach to utilize the known information on initial wind speed, time of day, FESS SOC, load level and conventional generation status at the start of the response time. The disturbance due to the loss of committed generating unit, load forecast uncertainty and wind power fluctuation within a lead time has been considered in the development of the disturbance model. Since transmission

systems are planned for N-1 contingency, a single outage will have negligible impact on the response ability of the system to any disturbances. As the failure rates of lines are comparatively low, the probability of multiple outages is insignificant within the short mission time given that the transmission system was healthy at the beginning of the mission. The contribution from the lines, are therefore, not considered in the disturbance model. However, the developed model can easily be extended to include these disturbances if desired. Figure 3.4 shows a general block diagram for the development of the proposed integrated disturbance model.

The development of the integrated disturbance model is described with an example of the IEEE-RTS connected to an 800 MW wind farm. The wind speed data from the North Dakota site is used in the study. An operating condition is considered with ten generating units selected from the loading priority table [31] to meet a load of 1450 MW at a time of day with a falling wind trend. It is assumed that a major contingency disturbance, D0 of 80 MW occurs due the forced outage of a generating unit. The initial wind power (IWP) at the time is 166 MW. The remaining healthy units must respond to recover the power deficit within a margin time of 10 minutes. In doing so, they must also respond to additional disturbances that can occur as a result of loss of other units, wind power fluctuations and load variations.

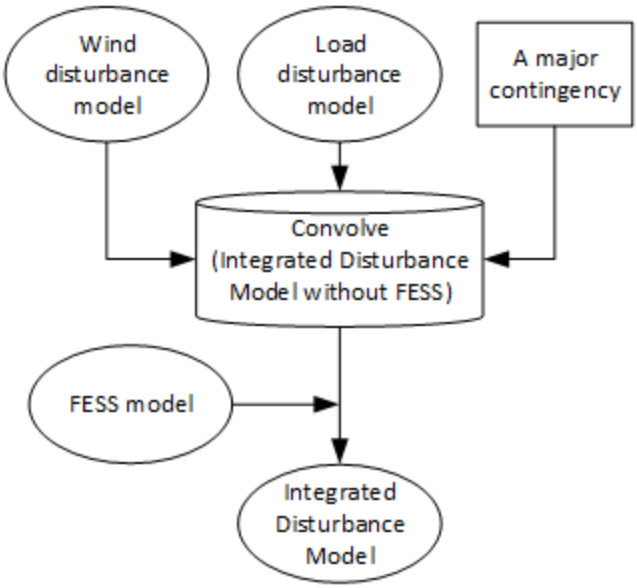

Figure 3. 4. Development of integrated disturbance model.

The impact of load uncertainty in unit commitment risk analysis are presented in [32-35]. It is a common practice to model the uncertainty by a normal distribution with a known standard deviation [10]. The load disturbance has been modeled using a 7-step discrete normal distribution with zero mean as expressed in (3.13) and shown in Figure 3.5 in this study. The standard deviation σ, which is a measure of spread in forecast error, will apparently be smaller for shorter forecast horizon [36]. A study on forecast errors in short-term load forecasting in utilities is presented in [37]. The study presented in this paper uses a σ of 0.5% of the mean value.

$$\mathcal{F}_L \sim P\left(D_j^{\sigma}\right) \tag{3.13}$$

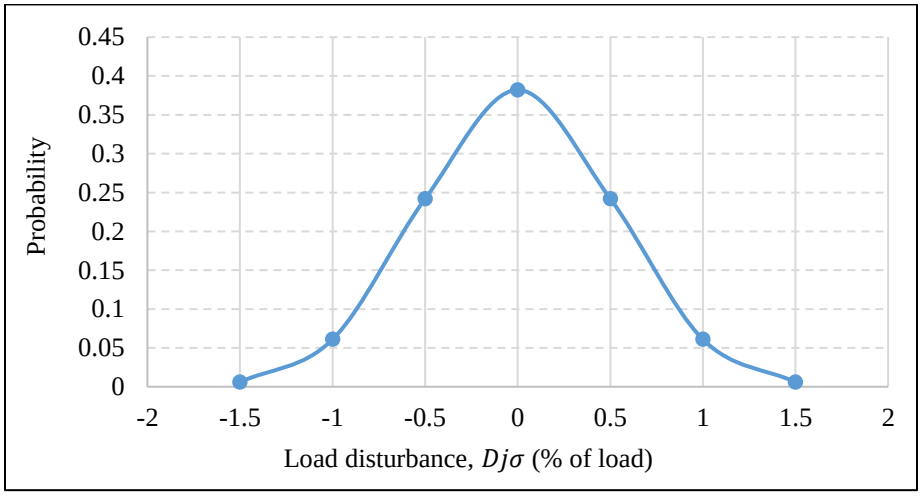

Figure 3. 5. Load Disturbance Model.

The disturbance due to wind power is modeled by a discrete probability distribution, $\mathcal{F}_{\omega}$, using the short-term wind modeling approach described in Section III considering the known conditions of the initial wind power, time of day and the margin time. The wind disturbance model is expressed in (3.14), in which the disturbance magnitude D_i^{ω} of the ith state is obtained from (3.15), and its corresponding probability from (3.16).

$$\mathcal{F}_{\omega} \sim P(D_i^{\omega}) \tag{3.14}$$

$$D_i^{\omega} = \mathrm{IWP} - \mathrm{WP_i} \tag{3.15}$$

$$P(D_i^{\omega}) = \mathrm{P}(\mathrm{WP}_i) \tag{3.16}$$

The load and wind disturbance functions, $\mathcal{F}_L$ and $\mathcal{F}_\omega$, are convolved to form an integrated disturbance model, $\mathcal{F}$ as expressed in (3.17). The integrated load and wind disturbance model for the margin time of 10 minutes is shown in Figure 3.6 with and without including the major contingency disturbance of 50 MW in the integrated disturbance model. The disturbance magnitude is expressed in percent of the system load.

$$\mathcal{F}(D = z) = \sum_{z_1=-3\sigma}^{3\sigma} \mathcal{F}_L\,(z_1)\,\mathrm{x}\,\mathcal{F}_\omega\,(z - z_1) \tag{3.17}$$

Where, $z_1 \in \{D^\sigma\}$ and $z - z_1 \in \{D^\omega\}$

It should be noted that a positive disturbance in Figure 3.6 represents a power deficit while a negative disturbance means excess power due to wind generation or load drops within the margin time. The magnitude, polarity and the probability of disturbance are the three important information obtained from the disturbance model. A large magnitude of positive disturbance tends to expose the system to a higher risk in responding to the deficit, whereas, a large negative disturbance can lead to the spillage of renewable energy if the system cannot adequately respond within the margin time to absorb the surplus energy. Figure 3.6 shows that the distribution plot shifts to the right when the major contingency is included in the model, showing increased power deficits with high probabilities.

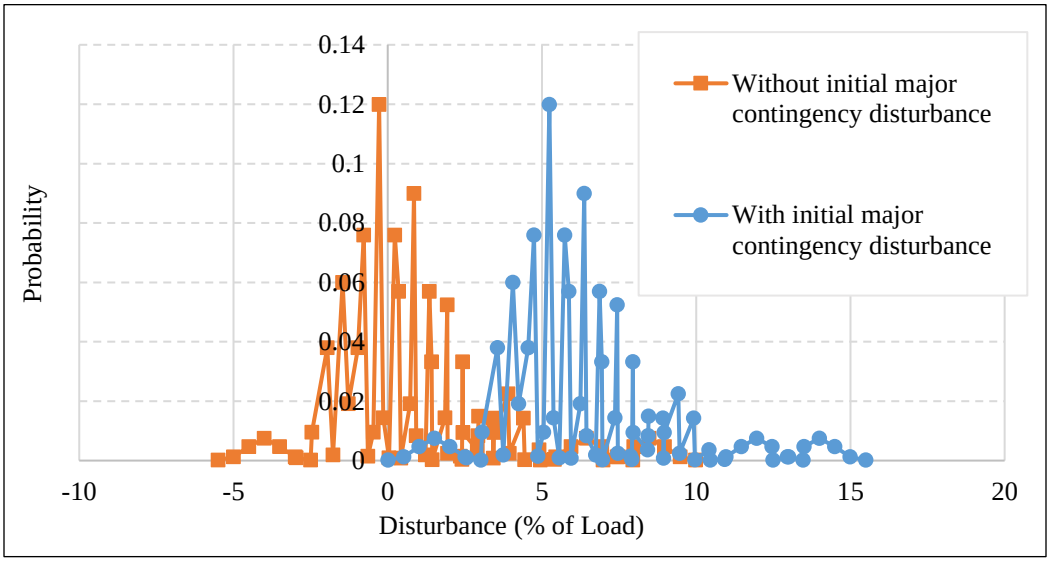

Figure 3. 6. Integrated disturbance model considering IWP of 166 MW in the falling trend, without FESS.

A FESS connected to the power system can absorb or mitigate the disturbances. The assisting capacity AsC of the FESS available to mitigate a disturbance of magnitude X can be obtained from the FESS SOC model described in Section II, and is expressed in (3.18), where $X = D_0 + D$, and D_0 and D are the magnitudes of the major contingency disturbance and the integrated load and wind disturbances respectively. A negative X indicates excess generation, and calls for a charging operation of the FESS, and vice-versa. A discrete probability distribution $\mathcal{F}_f$of the assisting capacity to the integrated disturbance is expressed in (3.19).

$$AsC = \begin{cases} -\min(P_{max}^{Dischrg},\ |X|; if\ X > 0 \\ \min(P_{max}^{Chrg},\ |X|; if\ X < 0 \\ 0; Otherwise \end{cases} \tag{3.18}$$

$$\mathcal{F}_f \sim P(AsC) \tag{3.19}$$

The integrated load and wind disturbance model is then convolved with the assisting capacity model of FESS to form an overall disturbance model, $\mathcal{F}'$ as expressed in (3.20).

$$\mathcal{F}'(D^f = z) = \sum_{z_1} \mathcal{F}_f\ (z_1)\ \text{x}\ \mathcal{F}_\omega\ (z - z_1) \tag{3.20}$$

Where, $z_1 \in \{AsC\}$ and $z - z_1 \in \{D\}$

The overall disturbance model is shown in Figure 3.7 considering an initial SOC of 60% of a FESS with a rated capacity of 300 MW at the time when the major contingency occurred. The initial SOC at the time of a major contingency mainly depends on the operating strategy employed by the FESS operator to fully exploit its capacity, energy and ramping capabilities. The disturbance models corresponding to 20% and 35% initial SOC are also shown for comparison.

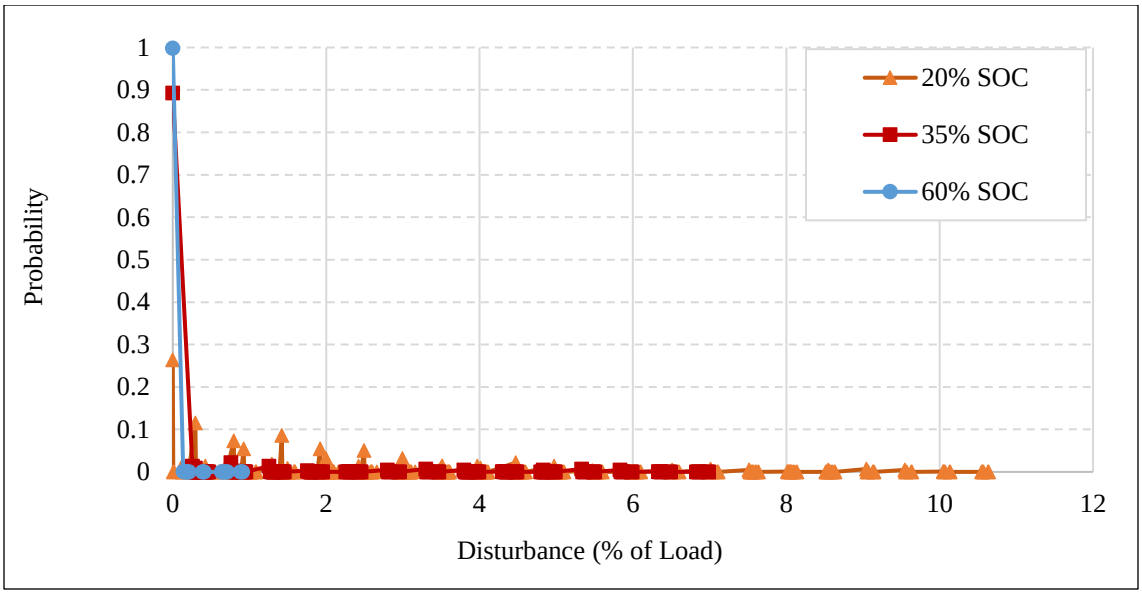

Figure 3. 7. Overall disturbance considering IWP of 166 MW (falling profile) with FESS.

The fast response ability of a FESS provides prompt assistance to mitigate unforeseen disturbances during power system operation. In the event when there is surplus energy from wind gusts, the additional energy can be quickly absorbed by the FESS. Figure 3.7 shows that the disturbance distribution shifts toward the "zero" disturbance axis with the increase in the initial SOC. A high initial SOC in the FESS at the time of major contingency helps the FESS to absorb the disturbance more effectively and improve the ability of the operating system to withstand disturbances, but limits the FESS's ability to capture surplus energy in a system with large wind penetration.

3.6. Response Risk Evaluation

A unit commitment based on economic load dispatch can lead to inadequate regulating margin if the operating costs of fast ramping units are relatively high at the load level. The regulating margin (RMi) of the ith unit is the portion of its spinning reserve (SRi) that can be available within a margin time MT as expressed in (3.21). The active capacity (ACi) of the ith unit is calculated using (3.22).

$$\mathrm{RM}_i = \mathrm{Min.}\,(\gamma_i \times \mathrm{MT}, \mathrm{SR}_i) \tag{3.21}$$

$$\mathrm{AC}_i \;=\; \mathrm{RM}_i + (\mathrm{C}_i - \mathrm{SR}_i) \tag{3.22}$$

Where, C_i and γ_i are rated capacity and ramp rate of the i^{th} generating unit.

The response risk (RR) is the probability that a system fails to respond adequately to a disturbance within the margin time to maintain the continuity of power supply [8], and can be expressed by (3.23).

$$RR = \sum_{j\epsilon\varphi_{\mathcal{F}}} RR_j \text{ x } \mathcal{F}'\,(D_j^f) \tag{3.23}$$

Where,

$$RR_j = \sum_{k\in\varphi_C} P_k \text{ x } Q_k \tag{3.24}$$

And,

$$Q_k = \begin{cases} 0; if\ \left(\sum_{i\in\varphi_G} AC_i\right) > \left|L_{net} + D_j^f\right| \\ 1; Otherwise \end{cases} \tag{3.25}$$

Where, $\varphi_{\mathcal{F}}$ is the set of all the states from the overall disturbance model expressed in (3.20), φ_C the set of combinations of outage contingencies of all the healthy generating units at the initial condition, P_k is the probability of the k^{th} contingency outage within the margin time, φ_G is the set of healthy generating units in operation under k^{th} contingency, and L_{net} is the net load obtained by subtracting the IWP from the system load.

An index designated as the response risk multiplication factor (RRMF) expressed in (3.26) is introduced in this paper to provide a relative measure of the impact of wind penetration on the response risk following a given major system disturbance.

$$\mathrm{RRMF} = \frac{RR_{\,wind,FESS}}{RR_{\,conv}} \tag{3.26}$$

Where, RR_{conv} is the response risk of the conventional system without considering wind power and FESS, and $RR_{wind,FESS}$ is the response risk of the system considering wind power with or without FESS.

3.7. Results and Analysis

The proposed approach to evaluate the response risk and RRMF is illustrated on the IEEE-RTS example described in Section IV with 10 conventional generating units scheduled to meet the 1450 MW load. An economic load dispatch based on first order gradient method [32] was performed for the net load of 1284 MW, considering 166 MW of wind generation from the 800 MW wind farm. The cost parameters provided in [38] were used in determining the economic load schedule for the ten committed units, and is presented in Table 3.2. The first six units, i.e. Unit 1 to Unit 6, are fully loaded and do not hold any spinning reserve or regulating margin.

It is assumed that a major contingency disturbance occurs due forced outage of Unit 8, which is dispatched at 80 MW. The remaining nine healthy units must respond to recover the power deficit within the margin time of 10 minutes. The generation response to the disturbance during the margin time is modeled by a cumulative probability distribution of the regulating capacity from the committed conventional generation. The cumulative probability distribution is created based on the concept presented in [10] and is presented in Figure 3.8 in terms of the active capacity (3.22) of available healthy units.

Table 3. 2. Economic schedule considering wind power.

Unit ID	Ci (MW)	Gmini (MW)	Schedule (MW)	RMi (MW)	ACi (MW)
1	50	0	50	0	50
2	50	0	50	0	50
3	50	0	50	0	50
4	50	0	50	0	50
5	400	200	346.95	0	346.95
6	400	200	347	0	347
7	350	150	150.05	90	240.05
8	197	80	80	60	140
9	197	80	80	60	140
10	197	80	80	60	140
Total			1284	270	1554

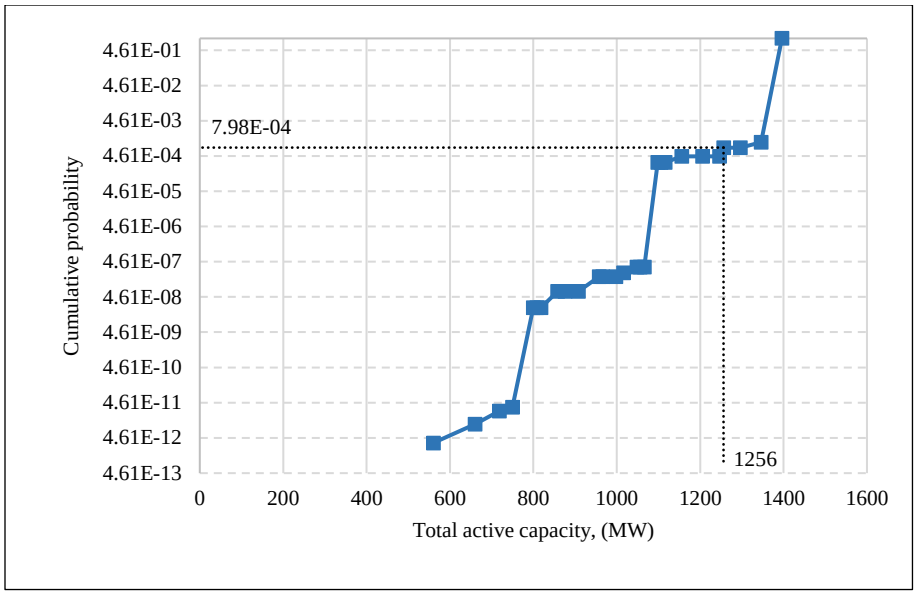

Figure 3. 8. Cumulative probability distribution of active capacities for different probable contingencies within margin time.

The overall disturbance model $\mathcal{F}'$ for this example is shown in Figure 3.7, which is represented by a discrete probability distribution of multiple disturbance magnitudes following the contingency. The horizontal line in Figure 3.8 illustrates the response risk associated with a selected state of the overall disturbance model following the contingency disturbance D_0 of 80 MW. The disturbance magnitude D_j^f for the selected state is 0 MW with a probability $P(D_j^f)$ of 0.264313 considering an initial FESS SOC of 20%. The committed generation must respond with a total active capacity exceeding |Lnet + D_j^f | = 1284 MW. Figure 3.8 shows that the response risk for the selected disturbance state is 7.98E-04. The expected response risk considering all the states of the overall disturbance model and their corresponding probabilities is 4.68E-04. This means that there is 0.0468% chance that the system including the FESS will fail to respond adequately to the loss of Unit 8 within the margin time.

In the similar manner, the response risk is found to be 6.80E-03 when the FESS is not considered in the previous example. The response risk without wind power and FESS in the example is 7.75E-04. The RRMF due to wind power is found to be 8.77. It implies that the integration of wind power to the IEEE-RTS makes the system nearly nine times more likely to fail in providing adequate response to contain the major contingency disturbance within the margin

time. The RRMF considering FESS with 20% SOC is found to be 0.60. This quantifies the impact of FESS in mitigating the increase in response risk due to wind power.

The results from the above example shows that the operating reliability quantified by the response risk of the system can degrade considerably with the integration of wind power. Another study was carried out to investigate the impact of increasing wind penetration and the application of FESS on the operating reliability. Figure 3.9 shows the variation of RRMF with increasing initial wind power (IWP) expressed in percentage of the load. Figure 3.9 also shows the RRMF when a 300 MW FESS is available in the system with initial 20% SOC at the time of the major contingency.

It should be noted that a RRMF equal to 1 indicates no change in the response risk of the system due to the addition of wind or ESS. The horizontal line corresponding to RRMF=1 in Figure 3.9 is used as the base line to compare the reliability impact of wind and FESS. The RRMF is plotted on a log-scale in Figure 3.9, and it increases significantly above the base line as wind power is increased, indicating degradation of the reliability of the committed operating system. The figure shows that the operating reliability can be improved relative to the base line with the use of FESS until the wind power exceeds 20% penetration. Beyond this point, the operating reliability cannot be maintained at the base level by the FESS although the RRMF is less than the case without FESS. It can be seen that regulating energy available from FESS is not sufficient to contain the disturbance and, consequently, RRMF decreases only slightly when wind penetration is 31% of the load.

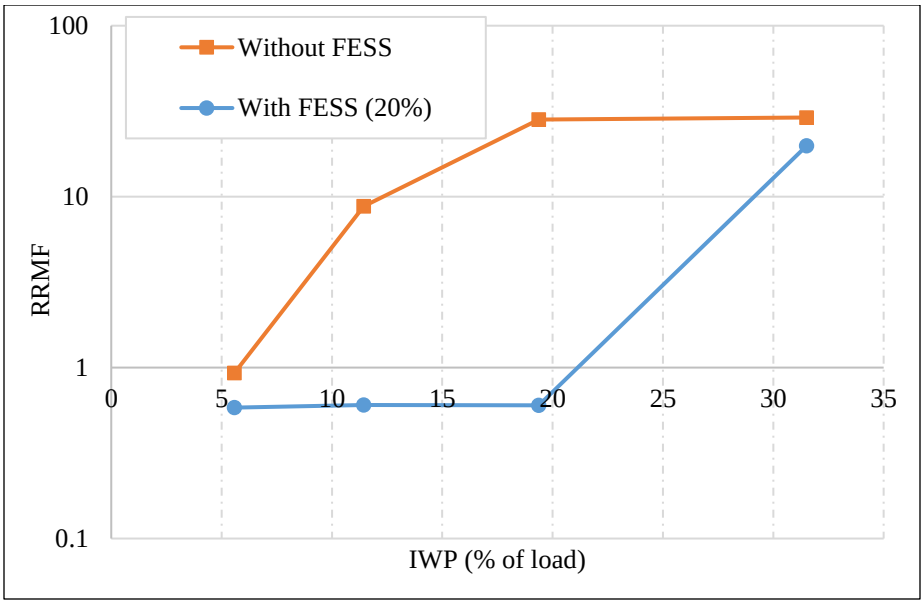

Figure 3. 9. RRMF with increasing wind power with and without FESS.

Another study was done to quantify the contribution of FESS to operating reliability following a major disturbance considering different SOC levels of the FESS at the time. The study considered two cases of major contingency disturbance: Case U8 is a sudden outage of Unit 8 dispatched at 80 MW as in the previous example and Case U1 is a sudden outage of Unit 1 rated and dispatched at 50 MW. It was assumed that the initial wind power was 31.5% of the load, and a 300 MW FESS was available to the system. The contingency was assumed to occur at a time when the wind had a falling trend. Figure 3.10 shows the variation of RRMF with initial SOC of FESS.

Figure 3.10 shows that the RRMF decreases with the increase in initial SOC of FESS for both major contingency disturbance cases. A higher SOC enables the FESS to provide more response capacity. Since SOC is expressed in percent of the rated FESS capacity, large capacity FESS will provide high regulating power and increased benefit in mitigating response risk. However, the appropriate FESS sizing should also consider benefits from other tasks or markets, such as frequency regulation, power quality, energy market and associated costs, in addition to responding to system contingencies. The results show that at least 30% SOC is required in the FESS to contain the disturbance due to Case U8. In Case U1, the FESS is not required to assist wind power as it has little impact on the response risk. The FESS however lowers the response risk below the base line in this case as shown in Figure 3.10.

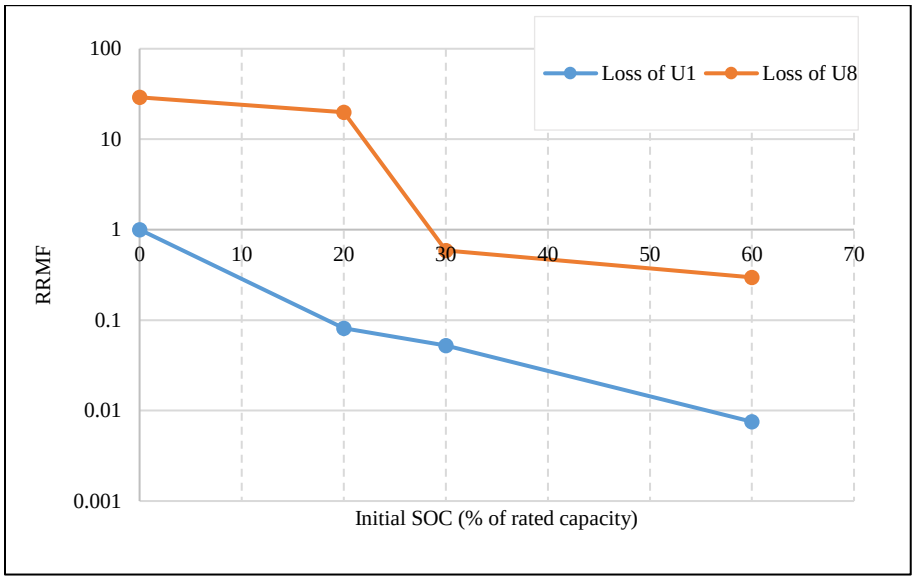

Figure 3. 10. RRMF considering different initial SOCs of FESS at the time of two major contingencies.

The evaluation in the above examples were done considering a falling wind trend. Another study was carried out to assess the operating reliability when a major contingency occurs during a rising trend. The study considered a sudden outage of Unit 8 dispatched at 80 MW in the operating schedule shown in Table II in the evening time when the wind has a rising trend. A 300 MW FESS with an initial SOC of 60% is available to the system. Figure 3.11 shows the variation of RRMF with initial wind power conditions with and without FESS. It can be seen that the RRMF decreases with the increase in IWP for both the cases. The RRMF curves for the two cases, i.e. with and without using FESS, almost coincide indicating little change in RRMF before and after using FESS. This is because the rising wind following the major contingency impacts the system in two ways; it lowers the positive disturbance magnitude reducing the response capacity requirement; and tends to raise the negative disturbance which is surplus energy eventually stored in the FESS to increase the regulating margin. The increase in FESS SOC after the system's response to the disturbance is also shown on the right axis of Figure 3.11. The initial SOC of FESS in this study is assumed to be 36 MWh (60% of rated capacity). Since FESS significantly reduces RRMF while charging during rising wind, the system can maintain acceptable operating reliability even with reduced regulating reserves during these times. The figure also shows the RRMF and FESS SOC

results for a falling wind trend for comparison. There is significant improvement in RRMF due to FESS under falling-wind condition as also shown in the previous example. The contribution of FESS to mitigating the operating risks comes at the expense of large drops in SOC of FESS as shown in Figure 3.11.

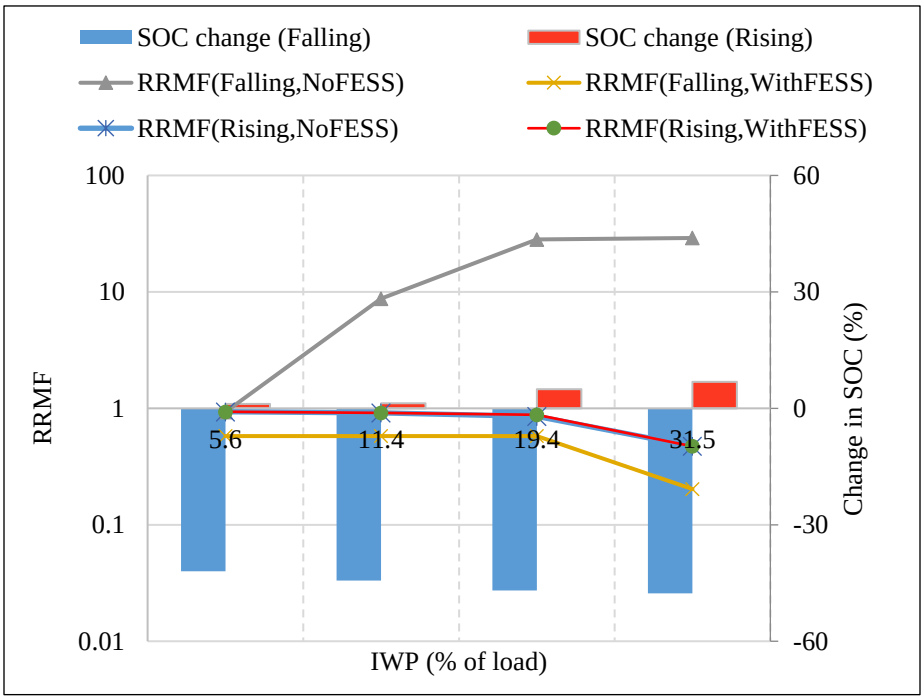

Figure 3. 11. RRMF and SOCs under diferent operating wind penetration levels considering rising / falling wind profile with / without FESS.

3.8. Conclusion

The ability of a power system to respond to major disturbances is severely limited by wind power intermittency, especially in operating systems with large wind penetration. High ramp rates of energy storage systems, such as FESS, allows them to provide prompt assistance to absorb the disturbances from the wind power fluctuations and load forecast errors within the response time following such major disturbances. This paper utilizes a probabilistic integrated disturbance model conditional upon the known conditions at the time of a major contingency disturbance to quantify the contribution of FESS on operational reliability of a wind-integrated system. The wind speed profile at the time of such major disturbance greatly influences the system's ability to respond to

the disturbance. If a major contingency event were to occur at the time when wind speed has falling-trend, the operational reliability degrades considerably as operating wind penetration is increased. An FESS used under such operating conditions can significantly improve the system's operating risk due to its stored regulating energy. On the contrary, the wind profile exhibiting the rising-trend at the time of a major disturbance boost's up the system's response and thus lowers the operating risk. The FESS can be used in such operating conditions to capture the additional wind energy while maintaining an acceptable operational reliability. The SOC of the FESS at the time of the disturbance dictates the extent to which it can assist the system, or avoid wind energy curtailments.

3.9. References

[1] P. Hu, "Reliability evaluation of generating systems containing wind power and energy storage," *IET Generation, Transmission and Distribution*, vol. 3, pp. 783–791(8), August 2009.

[2] "Global wind report annual market update 2016," Global Wind Energy Council, Brussels, Belgium, Tech. Rep., 2017.

[3] S. Ghosh and S. Kamalasadan, "An energy function-based optimal control strategy for output stabilization of integrated DFIG-Flywheel energy storage system," *IEEE Transactions on Smart Grid*, vol. 8, no. 4, pp. 1922–1931, 2017.

[4] N. S. Hasan, M. Y. Hassan, M. S. Majid and H. A. Rahman, "Review of storage schemes for wind energy systems," *Renewable and Sustainable Energy Reviews*, vol. 21, no. Supplement C, pp. 237 – 247, 2013.

[5] Suvire, "Active power control of a flywheel energy storage system for wind energy applications," *IET Renewable Power Generation*, vol. 6, pp. 9–16(7), January 2012.

[6] N. Abdel-Karim, D. Calderon, T. Coleman and J. Moura, "A hybrid probabilistic assessment using different renewable penetration scenarios in the north american bulk power system," in *Probabilistic Methods Applied to Power Systems (PMAPS), 2016 International Conference on. IEEE*, 2016, pp. 1–5.

[7] NERC, "NERC 2014 probabilistic assessment report," NERC, Tech. Rep., April 2014.

[8] A. Jain and R. Billinton, "Spinning reserve allocation in a complex power system," in IEEE PES Winter Meeting, 1973.

[9] N. A. E. R. Corporation, "Reliability standards for the bulk electric systems of north america," NERC, Atlanta, GA, Tech. Rep., 2013.

[10] R. Allan and R. Billinton, *Reliability evaluation of power systems*. Springer Science & Business Media, 1992.

[11] M. Fotuhi-Firuzabad, R. Billinton, and S. Aboreshaid, "Spinning reserve allocation using response health analysis," *IEE Proceedings-Generation, Transmission and Distribution*, vol. 143, no. 4, pp. 337–343, 1996.

[12] S.Thapa, "Operating risk analysis of wind integrated generation system," Ph.D. dissertation, Univ. Saskatchewan, Saskatoon, 2014.

[13] S. Thapa and R. Karki, “Reliability benefit of energy storage in wind integrated power system operation,” *IET Generation, Transmission & Distribution*, vol. 10, no. 3, pp. 807–814, 2016.

[14] R. Billinton, B. Karki, and R. Karki, “Unit commitment risk analysis of wind integrated power systems,” *IEEE Trans. Power Syst.*, vol. 24, no. 2, pp. 930–939, May 2009.

[15] T. Ding, C. Li, C. Yan, F. Li and Z. Bie, "A bi-level optimization model for risk assessment and contingency ranking in transmission system reliability evaluation," *IEEE Transactions on Power Systems*, vol. 32, no. 5, pp. 3803-3813, Sept. 2017.

[16] Z. Parvini, A. Abbaspour, M. Fotuhi-Firuzabad and M. Moeini-Aghtaie, "Operational reliability studies of power systems in presence of energy storage systems," *IEEE Transactions on Power Systems*, vol. PP, no. 99, pp. 1-1.

[17] P. Wang, Z. Gao and L. Bertling, "Operational adequacy studies of power systems with wind farms and energy storages," in *IEEE Transactions on Power Systems*, vol. 27, no. 4, pp. 2377-2384, Nov. 2012.

[18] X. Zhang and J. Yang, “A dc-link voltage fast control strategy for highspeed pmsm/g in flywheel energy storage system,” in *Electric Machines and Drives Conference (IEMDC), 2017 IEEE International Conference*, IEEE, 2017, pp. 1–7.

[19] R. Hebner, J. Beno, and A. Walls, “Flywheel batteries come around again,” IEEE spectrum, vol. 39, no. 4, pp. 46–51, 2002.

[20] S. Vazquez, S. M. Lukic, E. Galvan, L. G. Franquelo, and J. M. Carrasco, “Energy storage systems for transport and grid applications,” *IEEE Transactions on Industrial Electronics*, vol. 57, no. 12, pp. 3881–3895, 2010.

[21] M. I. Daoud, A. S. Abdel-Khalik, A. Massoud, S. Ahmed and N. H. Abbasy, "On the development of flywheel storage systems for power system applications: A survey," *2012 XXth International Conference on Electrical Machines*, Marseille, 2012, pp. 2119-2125.

[22] F. Deiana, A. Serpi, J. Abrahamsson, I. Marongiu and G. Gatto, “Extensive losses estimation of a novel high-speed permanent magnet synchronous machine for flywheel energy storage systems”, *2016 XXII International Conference on Electrical Machines (ICEM)*, Lausanne, 2016, pp. 1728-1734.

[23] P. Upadhyay and N. Mohan, “Design and FE analysis of surface mounted permanent magnet motor/generator for high-speed modular flywheel energy storage systems,” in *Energy Conversion Congress and Exposition, 2009. ECCE 2009. IEEE.* IEEE, 2009, pp. 3630–3633.

[24] R. Billinton and R. N. Allan, *Reliability evaluation of engineering systems*. Springer, 1996.

[25] C. Feinstein, P. Morris, and G. Hamm, "A review of reliability of electric distribution system components: Epri white paper," EPRI-1001873, California, 2001.

[26] D. of Defense, MIL-HDBK-217F-Reliability Prediction of Electronic Equipment, Washington, D.C., December 2 1991.

[27] [http://wind.nrel.gov/Web nrel/, accessed: July 2014.]

[28] R. Billinton, H. Chen, and R. Ghajar, "Time-series models for reliability evaluation of power systems including wind energy," Microelectronics Reliability, vol. 36, no. 9, pp. 1253–1261, 1996.

[29] H. A. Sturges, "The choice of a class interval," *Journal of the American statistical association*, vol. 21, no. 153, pp. 65–66, 1926.

[30] P. Giorsetto and K. F. Utsurogi, "Development of a new procedure for reliability modeling of wind turbine generators," *IEEE transactions on power apparatus and systems*, no. 1, pp. 134–143, 1983.

[31] P. M. Subcommittee, "IEEE reliability test system," *IEEE Transactions on Power Apparatus and Systems*, vol. PAS-98, pp. 2047–2054, 1979.

[32] F. A. El-Sheikhi and R. Billinton, "Load forecast uncertainty consideration in generating unit preventive maintenance scheduling for single systems," in *Probabilistic Methods Applied to Electric Power Systems, 1991, Third International Conference on. IET*, 1991, pp. 241–245.

[33] W. Li and R. Billinton, "Effect of bus load uncertainty and correlation in composite system adequacy evaluation," *IEEE Transactions on Power Systems*, vol. 6, no. 4, pp. 1522–1529, 1991.

[34] R. Billinton and D. Huang, "Effects of load forecast uncertainty on bulk electric system reliability evaluation," *IEEE Transactions on Power Systems*, vol. 23, no. 2, pp. 418–425, 2008.

[35] D. Zhai, A. Breipohl, F. Lee and R. Adapa, "The effect of load uncertainty on unit commitment risk," *IEEE transactions on power systems*, vol. 9, no. 1, pp. 510–517, 1994.

[36] E. Ciapessoni, D. Cirio and A. Pitto, "Effect of renewable and load uncertainties on the assessment of power system operational risk," in *Probabilistic Methods Applied to Power Systems (PMAPS), 2014 International Conference on. IEEE*, 2014, pp. 1–6.

[37] W. Bartkiewicz, Z. Gontar, J. S. Zielinski, and W. Bardzki, “Uncertainty of the short-term electrical load forecasting in utilities,” in *Neural Networks, 2000. IJCNN 2000, Proceedings of the IEEE-INNS-ENNS International Joint Conference on*, vol. 6. IEEE, 2000, pp. 235–240.

[38] R. R. Shoults and D. Sun, “Optimal power flow based upon pq decomposition,” *IEEE Transactions on Power Apparatus and Systems*, no. 2, pp. 397–405, 1982.

PREFACE TO CHAPTER 4: RECOVERY RISK ANALYSIS OF WIND-INTEGRATED COMPOSITE POWER SYSTEM WITH FLYWHEEL ENERGY STORAGE SYSTEM

This chapter is organized as a manuscript entitled "Recovery Risk Analysis of Wind-integrated Composite Power System with Flywheel Energy Storage System". The manuscript is submitted and is currently under review in IEEE *Transactions on Power Delivery.* The fundamental concept of generation response risk analysis used in Chapter 3 has been extended to incorporate role of transmission lines in the power system operating risk assessment. And therefore this chapter shares some of the literature and descriptions of component modelling with previous chapters. The work presented here is focused on quantifying the benefits of using FESS during the system operation and establishing a framework to evaluate the operating risk of wind-integrated composite power system. The final objective of the research, as stated in Section 1.5: 'to extend the fundamental concept of response risk analysis to address the locational impact of operational disturbances.

CHAPTER 4:RECOVERY RISK ANALYSIS OF WIND-INTEGRATED COMPOSITE POWER SYSTEM WITH FLYWHEEL ENERGY STORAGE SYSTEM

Saket Adhikari, Rajesh Karki, Senior Member, IEEE, Prasanna Piya, Member, IEEE

4.1. Abstract

With the increased uncertainty in the power system operation due to growing penetration of highly intermittent energy sources such as wind power, the need for the impact assessment of the renewable penetration on system operating risk and the quantification of benefits of using energy storage technologies is more than ever. A recovery-risk-analysis based analytical framework for operating risk assessment of wind-integrated bulk power system following a major contingency disturbance is presented in this paper. Two new risk indices that are essential to develop the recovery risk profile of the composite power system as well as individual bulk load delivery points following a major disturbance have been proposed in this work. The proposed framework aims to quantify the impact of increasing operating wind penetration on the system operating risk and quantify the reliability benefits of using fast-responding energy storage system such as flywheel energy storage system (FESS). The proposed methodology is illustrated through several case studies carried out in modified – Roy Billinton Test System.

4.2. Nomenclature

Ψ^B	Set of all busses
Ψ_j^B	Set of busses in neighborhood of j^{th} bus
Ψ^E	Set of states from FESS model
Ψ^W	Set of wind power states in wind power model
Ψ^F	Set of probable contingencies within margin time
λ	failure rate in failures / year
I	Mass moment of inertia in kg-m^2
P_{max}^{Chrg}	Maximum charging power in MW
$P_{max}^{Dischrg}$	Maximum discharging power in MW
SOC(t)	State of charge at time *t* in MWh
n_j^G	Number of generating units connected to jth bus
$\Phi_{i,j}^{g}$	Cost of i^{th} generating unit in j^{th} bus in $/MW
Φ^w	Cost of wind power in $/MW
Φ_j^{LC}	Cost of load curtailment at j^{th} bus
γ_{jk}	Susceptance of line connecting j^{th} and k^{th} bus in siemens
$g^{min}_{i,j}$	Rated lower limit of i^{th} generating unit in j^{th} bus in MW
$g^{max}_{i,j}$	Rated upper limit of i^{th} generating unit in j^{th} bus in MW
$P_{i,j,min}$	Permissible lower limit (within margin time) of i^{th} generating unit in j^{th} bus in MW
$P_{i,j,max}$	Permissible upper limit (within margin time) of i^{th} generating unit in j^{th} bus in MW
$\alpha_{i,j}/\beta_{i,j}$	Ramp up and down rate of i^{th} unit in j^{th} bus in MW/min
F_{jk}	Rated capacity of line connecting j^{th} and k^{th} bus in MW
t	Time
Δt	Time interval / Margin time
$\omega(t)$	Rotational speed of the flywheel at time t in rad/s
P_k	Probability of k^{th} SOC state from FESS model
P_{loss}	Power loss in flywheel

$p_{i,j}$	Power output of i^{th} unit in j^{th} bus in MW
LC_j	Load curtailed at j^{th} bus
L_j	Load at j^{th} bus
θ_j	Voltage angle at j^{th} bus in radians
WP	Wind power in MW
W_m	m^{th} state from wind power model in MW
w_k	Wind power that is being actually consumed as determined from load flow optimization under k^{th} contingency
$S_{i,j}$	Spinning reserve in i^{th} unit of j^{th} bus in MW
$P(D_k^F)$	Probability of k^{th} contingency from failure of one or more system components in MW
Q/Q'	Binary variable

4.3. Introduction

The objective of maintaining power balance in modern power system operation is increasingly challenged by the uncertainty in supply due to growing intermittent generation and random outages of generating units and transmission lines. These problems will be further aggravated as renewable energy penetration continues to increase in response to environmental concerns. The projected global trends of wind power growths [1] are raising concerns among power system operators regarding the reliability of system operation.

Power systems are operated with spinning and regulating reserves to mitigate any unforeseen disturbances within a specified time margin. The NERC standards, for instance, require that an immediate response should be available through automatic generation control (AGC) in order to maintain frequency and tie line regulation and the contingency reserve should be able to restore the system to its pre-disturbance state within 10 minutes of a disturbance in order to prevent load curtailment [2]. With the increased operating wind penetration (OWP), the share of conventional generation is reduced and the system gradually loses the inertial response. The reduced inertial response and increased variability and uncertainty in the system operation due to addition of intermittent energy source put the system operation in significant operating risk. In such situations,

energy storage system (ESS) can absorb the generation variability and mitigate transmission congestion, thereby improving the operational reliability and enabling further penetration of RES [3]. ESS with fast response capability such as flywheel energy storage systems (FESS) can ensure the desired prompt assistance during system operation to re-store the power balance within a short time-frame following a major contingency event.

Considerable work has been done in the past regarding system security assessment considering N-k contingency analysis [4-12]. Reference [4] ranks the contingencies based on performance index for a postulated list of contingencies using fast decoupled method. A fast contingency screening technique for generation system evaluation considering the severity and the probability of contingency is proposed in [5]. Reference [6] deals with day-ahead security management with respect to probable contingencies and ranks the contingencies based on line overloads. A novel approach for the power system security assessment using post-contingency security distance presented in [7] enables the system operators to know the available security margin after benign contingencies in addition to ranking the ones which cause overloads in the system. Similarly, [8] used Expected Power Not Served (EPNS) as a risk index for reliability evaluation in order to rank the contingencies and proposed a bi-level optimization model for risk assessment of transmission system. The reported literatures are mainly focused on the approach to identify the event(s) that harms the system operation the most in one way or the other. Reference [9] presents the fundamental idea behind generation response risk and proposes an approach for the risk evaluation. However, it exposes only the units with spinning reserve to the failure. Reference [10] improved on the approach and introduced a hybrid technique of adding deterministic security constraint in probabilistic framework for the response risk evaluation. The approach has limitation in its applicability in incorporating the role of transmission network in the system operating risk. For instance, even if the operating units maintain a reasonable amount of operating reserve, it would not guarantee the adequate response to the system disturbance if a critical line failure or congestion occurs. Similarly, [11] presented a simulation-based approach for operational adequacy analysis of wind-integrated power system and sums up the operational risk in terms of expected energy not served (EENS) in the time horizon of months. A more general framework to perform the similar task as in [11] was presented in [12] and it evaluated the operational risk in terms of UCR and EENS. Although [11] and [12] provided the important tool to establish a comparatively long-term operational risk profile which is useful for the system

planners, it has limited significance in terms of analysis of the ability to recover from the major contingency disturbances within a definite short time frame. Furthermore, the work presented in the literature assumes that committed units are connected to an ideal common bus serving the total system load at the bus and thus neglects the constraints imposed by the transmission network and the locational dispersion of the generation and load points within the network in the risk evaluation process, which is an important consideration in a bulk power system (BPS) operation. The impact of a major contingency perceived from the bulk system's perspective can be different from a load delivery point's perspective, and the impacts can vary considerably among the different load delivery points. It is also necessary to take into account the ramping abilities of the generating units while evaluating the severity of the contingencies. The evaluation frameworks in the reported literature do not offer flexibility to incorporate and assess the role of ESS in enhancing the power system operational reliability. However, with the current growth rate of renewable injection into the power system, it becomes more important to assess the system's ability to respond toward different contingencies within limited time-frame.

This paper presents a new framework designated as the recovery risk analysis of BPS, which can analyze time-bound response of committed generation units, located throughout the network, to respond to supply/demand and network disturbances, and regain the power balance at each bulk delivery point. The developed framework offers the flexibility to accommodate time-dependent wind variation models and the operating reliability model of FESS. The framework can therefore be used to explore the potential of FESS in maintaining the system operation within reasonable operating risk. The paper presents a margin time disturbance model (MTDM) to represent the probable disturbances that may arise within the margin time (MT) following a major contingency, which is an important consideration in modern power system operation, but is overlooked by the reported works. The margin time disturbances can come from generation loss, line outages and/or wind power fluctuation that hinder the system's effective generation response capacity in mitigating the original major contingency. The developed framework can be used to create the risk profile of BPS as well as its individual bulk load points following a major contingency which helps to assess the locational impact of the contingency within the system during the system operation.

The probability of a power system being unable to reinstate the power balance at the bulk delivery nodes within a definite time-frame following a major contingency is defined as recovery risk in this paper. In addition to generating units' responses, the constraints imposed by the

topology of power system at the bulk load points are also considered in a recovery risk assessment. Two operating risk indices, namely system recovery risk (SRR) and load point recovery risk (LPRR) have been proposed. The LPRR measures the probability of a bulk load point not being able to recover from upstream network or supply disturbance within acceptable time, whereas, the SRR measures the same from the overall system's perspective. The LPRR profile of different load points with reference to the SRR of the BPS helps to identify the individual load point's share in the system operating risk, which helps to prioritize the use of FESS to mitigate the risks. The recovery risk analysis using the LPRR and SRR of a wind-integrated BPS helps to measure the relative change in the operating risks in the BPS as well as the bulk load delivery points, as a result of increasing OWP levels with/without the presence of FESS. And thus it quantifies the impact of increasing OWP on the power system operating reliability as well as the reliability benefits of FESS in the wind-integrated BPS operation.

4.4. Reliability modelling of system components

The operating characteristics of generating units and transmission lines of a BPS are represented by two–state Markov models [9]. In the operating domain of a power system reliability study, the outage probability of the components is not a static-characteristic, but rather is time-dependent. The probability of a component failing in a mission time Δt given that it was operating successfully at the beginning of mission is known as its outage replacement rate (ORR) [9], and can be obtained using (4.1).

.

$$ORR(T)=1-e^{-(\lambda_{eqv})\Delta t} \quad (4.1)$$

A conditional probability approach has been used in this paper to obtain a short-term wind speed model following a major contingency disturbance conditional upon the known conditions prior to the disturbance. The known wind conditions are the initial wind speed (IWS) at the time t when the contingency just occurred, and the time of day of such occurrence lying in the rising, falling or flat trend of the historical wind profile. For a given value of IWS at a time t, a set of data on wind speed at subsequent interval Δt can be obtained either from historical wind speed data or from a series of synthetic data from a statistical model, such as ARMA [13], in the absence of

adequate historical data. Using Sturges' rule [14], the data set can be categorized into a fixed number of intervals each of which being represented by the mid-point of the interval. The frequency of occurrence of the wind speeds within the different intervals from the data set corresponding to different IWS can be used to create a discrete probability distribution of wind speeds conditional upon given IWS called as conditional wind speed distribution (CWSD).

Figure 4.1 shows CWSD for subsequent interval of 10 minutes for a given IWS of 28 km/h during the time of day when wind speed profile is exhibiting falling and rising trend. The CWSD can be transformed into conditional wind power distribution (CWPD) using Wind Turbine Generator (WTG) power curve characteristics [13]. Wind speed data obtained from the National Renewable Energy Laboratory (NREL) [15] collected at 10 minute time intervals for a site in North Dakota over a period of three years are used in this work, which exhibits a typical diurnal-characteristics of rising, flat / falling trend.

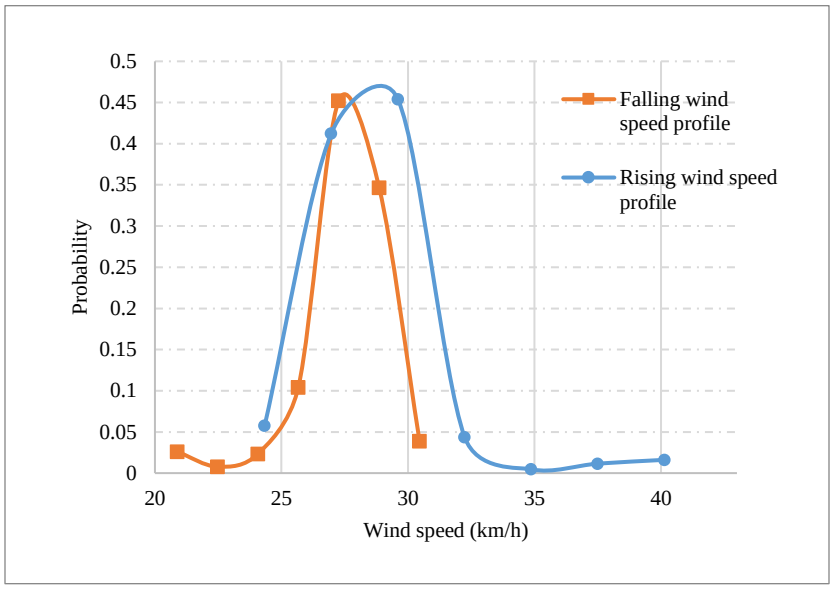

Figure 4. 1. CWSD for IWS of 28 km/h considering falling and rising trend in wind speed profile.

A flywheel stores energy in the form of mechanical energy determined by the speed of its rotating mass. The SOC of a FESS is the amount of energy stored at a given time, and can be obtained using (4.2).

$$SOC(t) = \frac{1}{2} I \times [\omega(t)]^2 \qquad (4.2)$$

Magnetic bearing system and a vacuum enclosure provides a near-frictionless environment for the rotor's rotation. A permanent magnet synchronous machine operates in both motor and generator modes. The machine is enclosed inside a vacuum chamber, and a dedicated cooling system is provided to dissipate the heat generated. A back-to-back converter connected with each flywheel facilitates the power exchange between the flywheels and the grid. A power control module (PCM) keeps track of the SOC and state of health of the associated flywheel. A typical FESS plant will have multiple clusters grouped together to meet the required power and energy capacity, as shown in Figure 4.2. Each cluster is provided with a cluster controller that keeps track of SOC of FESUs in the cluster and also applies operational logic to make the power exchange between the cluster and the grid.

An integrated reliability model of a FESS incorporating its specific charge/discharge, storage and failure characteristics is presented in [16], in which a discrete probability distribution of the state of charge (SOC) of the FESS plant is created. Table 4.1 shows the SOC model of FESS for a 10-minute mission time conditional upon the initial SOC of each flywheel being 50% of SOC_{rated} and the components being fully functional at the start of the mission. The model considers a FESS plant constituting 60 clusters of 10 flywheels each with power rating (P_{rated}) and energy rating (SOC_{rated}) of 0.5 MW and 100 kWh respectively. The data on failure rates of different system components needed in the modeling were obtained from [17, 18].

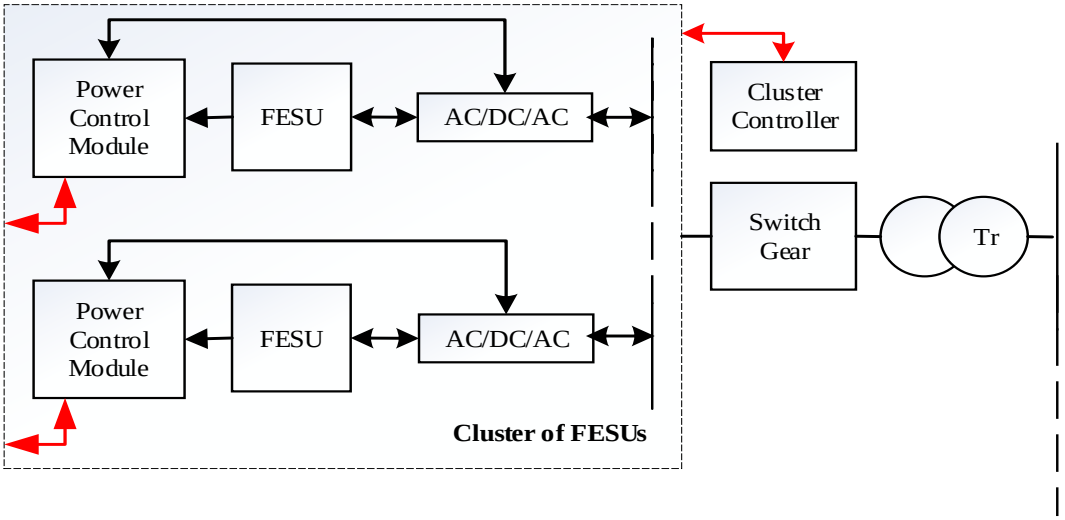

Figure 4. 2. Simplified layout of a cluster of FESUs in a typical FESS plant.

Table 4. 1. State of charge model.

State #, k	SOC (MWh)	Probability, Pk
1	30	0.96059
2	29.95	0.03838
3	29.9	0.00077
-	-	-
-	-	-
-	-	-
28	0	2.09E-07

A FESS can be used to absorb or mitigate the disturbances. The assisting capacity C of the FESS to mitigate a disturbance of magnitude X can be obtained from the FESS SOC model presented earlier, and is expressed in (4.3). A negative X represents excess generation, and calls for a charging operation of the FESS, and vice-versa.

$$C = \begin{cases} -\min(P_{max}^{Dischrg},\ |X|; if\ X > 0 \\ \min(P_{max}^{Chrg},\ |X|; if\ X < 0 \\ 0; Otherwise \end{cases} \quad (4.3)$$

The new SOC of the flywheel after charging / discharging or being in stand-by for Δt duration can be evaluated using (4.4).

$$SOC(t+\Delta t) = SOC(t) + \gamma \text{ x } P(t) \text{ x } \Delta t - \int_t^{t+\Delta t} P_{loss}\, dt \quad (4.4)$$

Where, $P(t)$ is the power available to charge or discharge, and γ = {1, -1, 0} for charging, discharging and stand-by operation respectively during the interval Δt. The loss power P_{loss} is a function of rotational speed of the flywheel. A detailed study in estimation of different types of losses and empirical expressions for losses with respect to speed are presented in [19] – [21]. For charging operation, $P(t) \leq P_{max}^{Chrg}$, and for discharging operation, $P(t) \leq P_{max}^{Dischrg}$. Maximum charging power P_{max}^{Chrg} is limited to power rating of the generator, while the maximum discharging power, $P_{max}^{Dischrg}$ is given by (4.5).

$$P_{max}^{Dischrg} = \min\left\{P_{rated}, \frac{SOC(t)\text{-}SOC_{min}+Loss}{\Delta t}\right\} \quad (4.5)$$

4.5. Methodology

The methodology for recovery risk assessment of composite power system is illustrated in the flowchart as shown in Figure 4.3. The committed generating units are dispatched based on DC optimal power flow (OPF). The IBM optimization studio [22] integrated in MATLAB environment was utilized in this work for performing DC OPF. The objective function for the DC-OPF is formulated as shown in (4.6), and the constraints are expressed in (4.7) – (4.12).

$$\sum_{j\in\Psi^B}\left[\left\{\sum_{i=1}^{n_j^G}\Phi_{i,j}^{g} \text{ x } p_{i,j}\right\} + \Phi^{w} \text{ x } WP + \Phi_j^{LC} \text{ x } LC_j\right] \quad (4.6)$$

$$\sum_{j=1}^{\Psi^B}\left[WP + \sum_{i=1}^{n_j^G} p_{i,j} - \sum_{k\in\Psi_j^B}\gamma_{jk} \text{ x } (\theta_j - \theta_k) + LC_j\right] = 0 \quad (4.7)$$

$$0 \le LC_j \le L_j \quad (4.8)$$

$$-\pi \le \theta_j \le \pi \quad (4.9)$$

$$0 \le WP \le IWP \quad (4.10)$$

$$-F_{jk} \le \gamma_{jk} \text{ x } (\theta_j - \theta_k) \le F_{jk} \quad (4.11)$$

$$g^{min}_{i,j} \le p_{i,j} \le g^{max}_{i,j} \quad (4.12)$$

Based on the knowledge of initial wind power (IWP) and the present load, the committed units are dispatched based on DC-OPF. A major contingency to be analyzed is introduced, which marks the beginning of MT for recovery risk (RR) evaluation. Such contingency can arise from forced outage of system component(s); mainly generating units and major transmission lines.

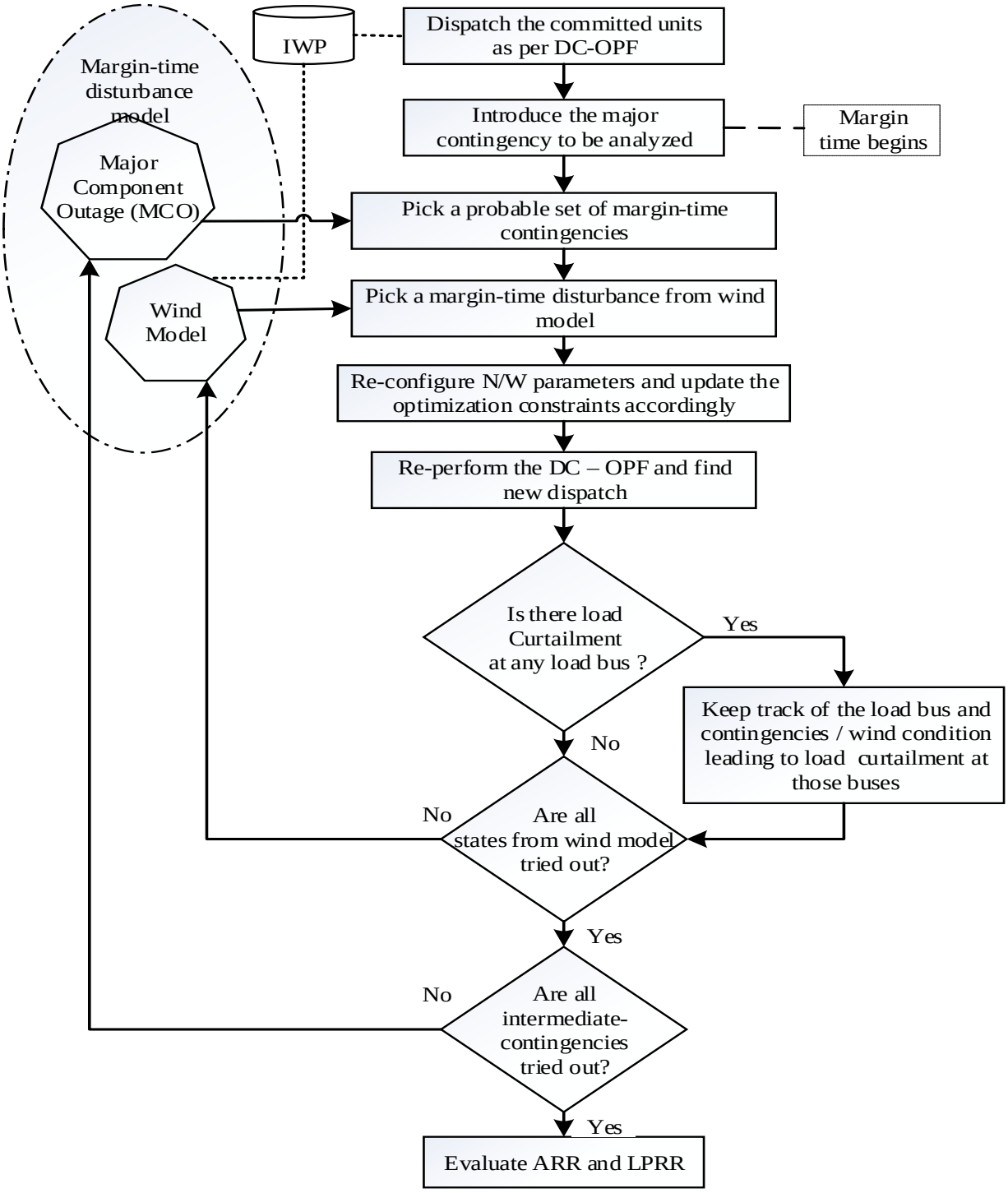

Figure 4. 3. Methodology to evaluate recovery risk of composite power system.

The system responds to maintain the power balance at all the bulk load points within the MT following the major contingency disturbance. The responding resources are subject to further

disturbances due to outages of healthy components, wind power fluctuations and load variations within the MT. The magnitudes of load variations within a short MT of about 10 minutes are relatively small compared to disturbances from wind power and component failures, and are therefore, not considered in the evaluation. The MTDM shown in Figure 4.3 consists of "major component outages (MCO)" and "wind disturbance". The disturbances due to outage of operational generating unit and major line within the MT are considered in the MCO. A system with N such components will consist of 2^N contingencies considering a two-state Markov model representation of each component. These contingencies can be enumerated in a recursive technique by bit-flipping an N-bit binary number in a sequence. Numbers in decimal system starting from 2^N-1 down to zero can be converted to N-bit binary system. The starting number in binary format will have all bits set to 'high' representing that all major components available and each subsequent number will have one additional bit flipped to 'low' representing one or more major component being down. This technique is incorporated in the MCO shown in Figure 4.3. A suitable strategy can be applied to reduce the number of contingencies in the MCO. A simple approach is to limit the order of contingencies to exclude contingencies with low probability. Similarly, the probability of a contingency or impact of a contingency or both can be used as criterion to limit the number of probable contingencies to save the computational burden without compromising the accuracy of the evaluation results.

A state from the multi-state wind model conditional upon the IWP is picked, to account for probable disturbance coming from the wind during the MT. The new system-state based on the probable disturbances is re-defined and the objective function (4.6) is re-optimized with new system constraints and updated parameters. The constraints (4.10) and (4.12) are modified to (4.13) and (4.14) respectively, while the rest remain unmodified.

$$0 \leq \mathrm{WP} \leq \mathrm{W_m} \tag{4.13}$$

$$P_{i,j,min} \leq p_{i,j} \leq P_{i,j,max} \tag{4.14}$$

Where,

$$P_{i,j,max} = Minimum\left\{S_{i,j} + \alpha_{i,j} \times \Delta t,\ G_{i,max}\right\} \tag{4.15}$$

$$\mathrm{P_{i,j,min}} = \mathrm{Maximum}\left\{\mathrm{S_{i,j}} - \beta_{i,j} \times \Delta t,\ \mathrm{G_{i,min}}\right\} \tag{4.16}$$

Since the dispatched units cannot fully swing their output within the rated limit in the short margin time Δt, the bounds in corresponding generating units are determined by their respective ramp rates and the spinning reserve, as expressed in (4.15) and (4.16).

It is vital to note that the cost of load curtailment Φ_j^{LC} in load bus is set to very high value to make sure that load curtailment happens in any load bus as only last resort. The costs in different buses can be varied in order to set priority among the buses regarding the load curtailment if the operator wishes.

For every re-dispatch option corresponding to each probable system state within margin time, the set of events (lines / generating units failure and wind state) leading to the load curtailment at any bus are noted to evaluate system recovery risk (SRR) and load point recovery risk (LPRR) as expressed in (4.17) and (4.18) respectively.

$$SRR = \sum_{k\in\Psi^F}[\, P(D_k^F) \text{ x } \{\sum_{m\in\Psi^W} P(W_m) \text{ x } Q\}\,] \tag{4.17}$$

$$LPRR = \sum_{k\in\Psi^F}[\, P(D_k^F) \text{ x } \{\sum_{m\in\Psi^W} P(W_m) \text{ x } Q'\}\,] \tag{4.18}$$

Where,

$$Q = \begin{cases} 1, & \sum_j LC_j > 0 \\ 0, & Otherwise \end{cases} \tag{4.19}$$

$$Q' = \begin{cases} 1, & LC_j > 0 \\ 0, & Otherwise \end{cases} \tag{4.20}$$

When wind power suddenly grows during system operation, the committed conventional generation units tend to ramp down to allow more wind into the system. Due to ramping down constraints and/or the lower permissible limit of some units, there is always a chance of some wind-spillage. The expected wind spillage (EWS) during system operation is evaluated using (4.21). Apparently, EWS obtained from (4.21) will be very small owing to the small evaluation time of 10 minutes.

$$EWS = \sum_{k\in\Psi^F}[\sum_{m\in\Psi^W}(W_m - w_k) \text{ x } P(W_m)] \text{ x } P(D_k^F) \tag{4.21}$$

Once the load point with poor recovery risk profile is identified, it can be re-enforced using the FESS. In this paper, FESS is operated to assist the load bus identified from the risk analysis, whenever there is load curtailment at the bus and also to store the surplus wind in the system if any. The expressions for risk indices in (4.17) and (4.18) can be easily modified to incorporate the

FESS model developed in Section 4.4 using conditional probability approach, as shown in (4.22) and (23) respectively. In this case, the value of LC_j in (4.19) and (4.20) is evaluated using (4.24). The parameter 'C' is obtained from (4.3). Similarly, the expression of EWS from (4.21) will change to (4.25).

$$SRR = \sum_{k \in \Psi^E} SRR_k \text{ x } P_k \quad (4.22)$$

$$LPRR = \sum_{k \in \Psi^E} LPRR_k \text{ x } P_k \quad (4.23)$$

$$LC_j = LC_j + \min (LC_j, LC_j + C) \quad (4.24)$$

$$EWS = \sum_{k \in \Psi^E} EWS_k \text{ x } P_k \quad (4.25)$$

In above expressions, SRR_k, $LPRR_k$ and EWS_k corresponding to k^{th} state of FESS model are obtained from (4.17), (4.18) and (4.21) respectively.

4.6. Results and analysis

Proposed methodology is applied to modified - Roy Billinton Reliability Test System (RBTS) shown in Figure 4.4. The details of capacities and failure rates of the lines are shown alongside the lines in Figure 4.4, while rest of the parameters remain same as in standard RBTS. The calculations have been presented in per unit system with base value of 100MW and the generation capacity loss of a 0.2 p.u has been used as an example to represent the major contingency disturbance to which the system responds within the margin time (MT) of 10 minutes.

A study was carried out to illustrate the evaluation of proposed risk indices of the test system. Based on N-1 contingency, nine units are selected from standard loading order [23] to meet the system load level and the system's recovery risk for the margin time of 10 minutes following the major contingency is investigated. For this study, wind power has not been considered. Table 4.2 shows the SRR and LPRR evaluated for different buses in the system. The LPRR at Bus 2 is almost zero and LPRR at Bus 4 and Bus 5 are very small compared to Bus 3. This implies that for the sudden loss of 0.2 p.u. capacity, the risk of having load curtailment at Bus 2 is near zero, while the risk at Bus 3 is significantly higher than that of other load busses. The LPRR of 0.000593 at Bus 3 indicates that there is 0.059% chance that the healthy committed units will not be able to crank-up the generation to meet the load demand of 0.8 p.u. at Bus 3 within 10 minutes MT after the major contingency. The value of SRR is seen very close to the LPRR of Bus 3. Since the LPRR at

the rest of the buses is very small compared to that at the Bus 3, it is apparent that SRR will be very close to LPRR of Bus 3. It means the poor performance at Bus 3 contributes to SRR the most. The study points out the Bus 3 as the weakest-link in the network and thus needs enhancement. It should be noted that Bus 3 has largest load level of 0.85 p.u. Thus, it needs to be answered if the poor performance is linked with the load level at the bus or the system topology.

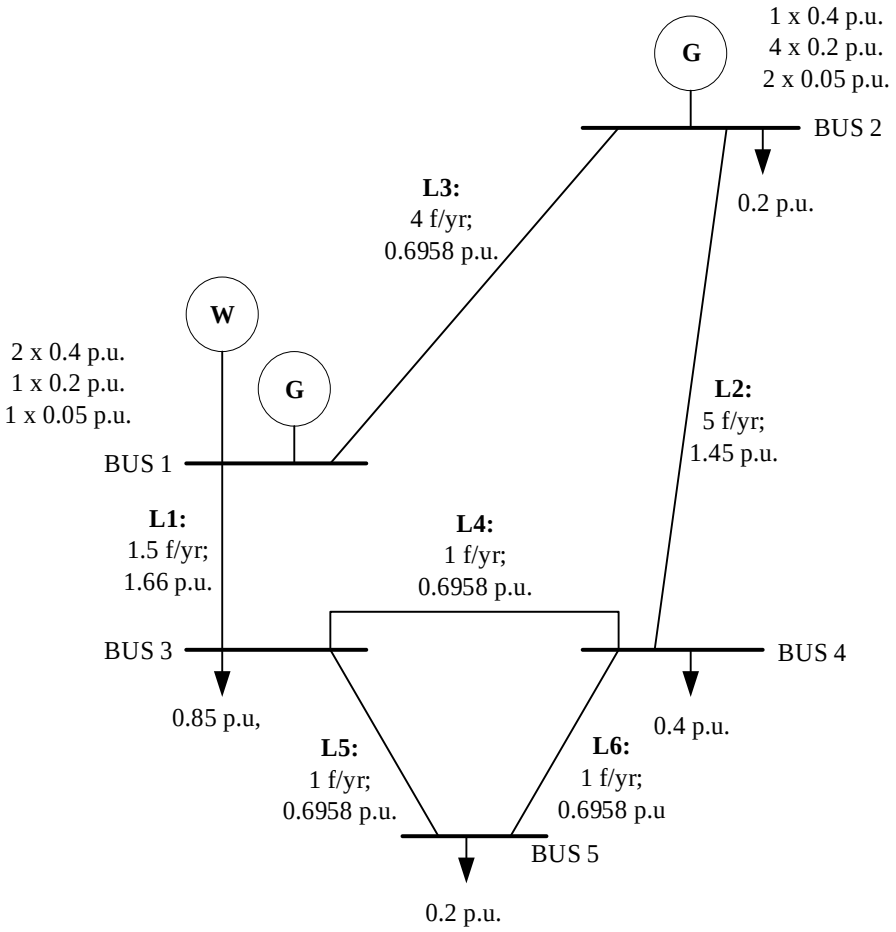

Figure 4. 4. Modified Roy Billinton Test System.

Table 4. 2. SRR and LPRR at different busses.

LPRR at bus:				SRR
2	3	4	5	
0E-08	0.00059342	1E-08	1E-08	0.00059343

Figure 4.5 shows the operating risk profile of different load points and the system for a sudden loss of 0.2 p.u. generation capacity, while the load level at Bus 3 is varied from 0.35 p.u. to 0.85 p.u. Two important observations from Figure 4.5 are: first, for the entire range of load level, the LPRR at Bus 3 is higher compared to other busses and second, the plot for LPRR at Bus 3 is almost coincident with SRR plot. It is thus consistent with the previous observation that the major contributor of the system recovery risk (SRR) is Bus 3 and additionally, the poor risk profile of Bus 3 comes from the network topology rather than the load level itself. The observations is further justified if we note the failure rate of the lines in the test system network. Higher failure rates of lines 1 and 3 makes the higher order contingencies leading to load curtailment at Bus 3 more probable than at other load points.

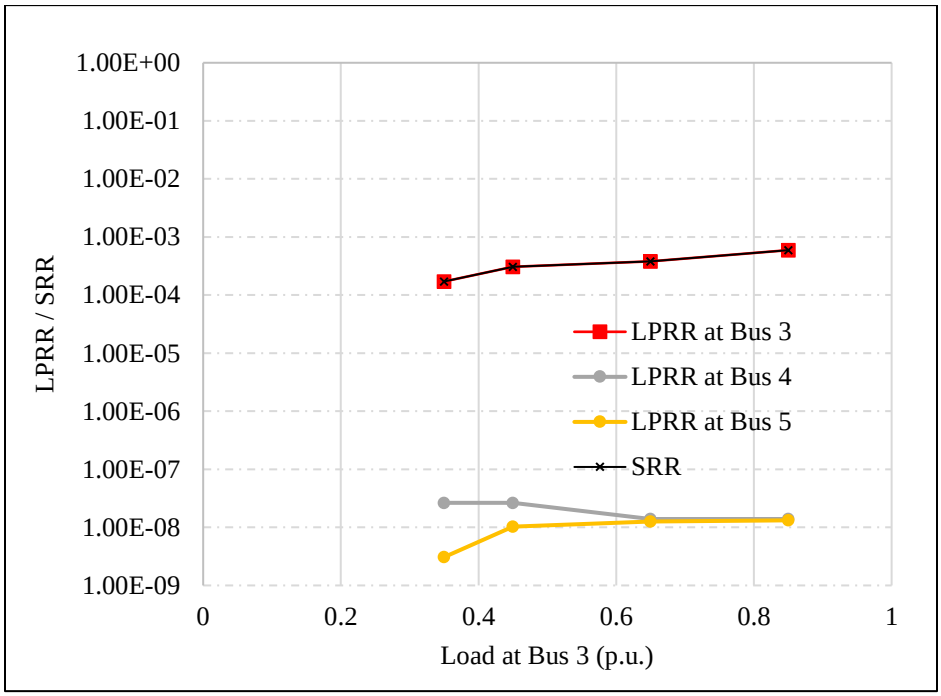

Figure 4. 5. Recovery risk profile for a range of load level at Bus 3.

The following study was done to see how the risk profile is further degraded by increasing operating wind penetration (OWP). A wind farm with installed capacity of 2.5 p.u. is connected to Bus 1 as shown in Figure 4.4. In this study, the IWP has not been incorporated in the unit commitment (UC) which results in fixed number of committed-generating units for a system load regardless of magnitude of IWP and the UC has been termed as fixed unit commitment (FUC).

Figure 4.6 shows the recovery risk profile of different load points and system considering several IWP. The wind speed is assumed to have a falling trend at the time of the major contingency. For smaller IWPs at the beginning, the risk indices have nearly constant values with slight decrement. The overall risk profile has the increasing trend with the IWP. Due to FUC, more reserve margin (RM) becomes available as IWP is increased. Initially, the disturbances resulting from the wind power fluctuation is subdued by the increased RM and hence the small dips in the risk profile at the beginning. However, as the IWP increases, the risk profile degrades since the disturbances coming from the wind power fluctuations become dominant. When the IWP is significantly large, the amount of RM available in the committed units become so high that the risk profile drops again. Importantly, the LPRR profile at Bus 3 is again dominant compared to other load points and is almost coincident with SRR profile.

Discarding the IWP during UC, usually results in over-commitment of the conventional generating units. A study was done incorporating the IWP in the UC and the resulting recovery risk profile is presented in Figure 4.7. In this case, as IWP is sufficiently increased, less number of conventional units are committed to meet the system load. In this modified unit commitment (MUC), when IWP is increased, RM does not increase proportionally and consequently the recovery risk profile degrades severely as shown in Figure 4.7.

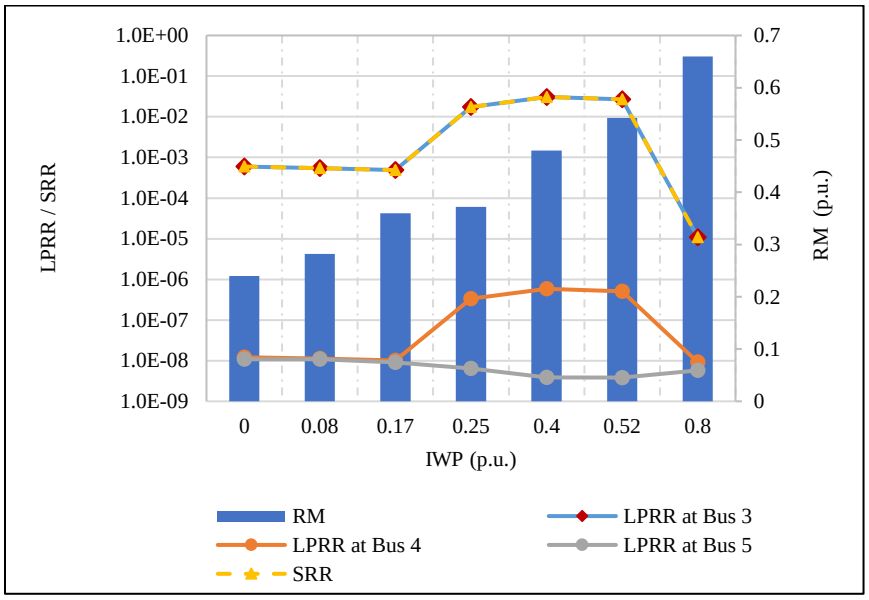

Figure 4. 6. Recovery risk profile with different IWP considering fixed unit commitment with falling trend in wind speed at the time of major contingency.

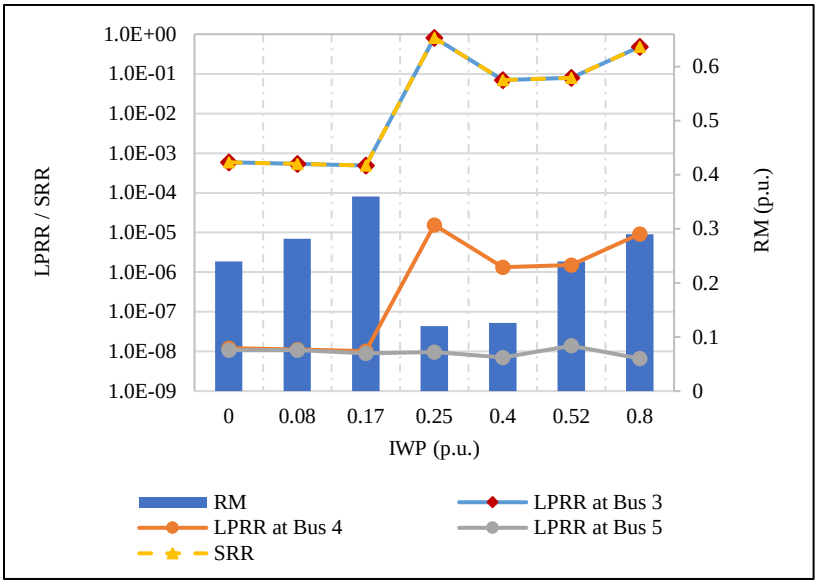

Figure 4. 7. Recovery risk profile with different IWP considering modified unit commitment with falling trend in wind speed at the time of major contingency.

The following study was done considering the rising trend in wind speed profile at the time of major contingency, to assess the impact of rising trend of wind speed in the recovery risk. Figure 4.8 shows the recovery risk profile and RM available in the system at various OWP levels, assuming the rising trend in wind speed profile at the time of major contingency. Under FUC, when IWP is increased, RM increases proportionally. With the increased likelihood of having surplus wind power, the risk profile improves with increasing the IWP. However, under MUC RM does not increase proportionally with increasing IWP and therefore, the increased chances of surplus wind power is not sufficient to overcome the increased disturbances from the wind power. Consequently, the risk profile is seen to degrade with IWP.

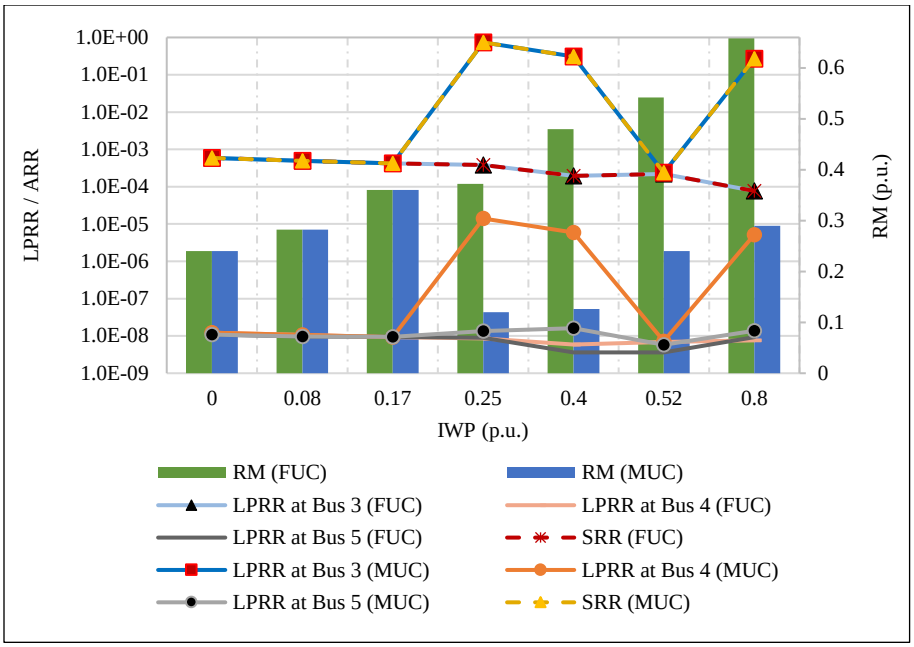

Figure 4. 8. Recovery risk profile with different IWP considering MUC and FUC with rising trend in wind speed at the time of major contingency.

The LPRR profile at Bus 3 is found to be coincident with SRR profile of the system in all of the studies discussed earlier, pointing out Bus 3 to have a poor recovery risk profile. Following study was carried out to quantify the reliability benefits of FESS. In this study, a FESS plant constituting 60 clusters of 10 flywheels each with power rating (P_{rated}) and energy rating (SOC_{rated}) of 0.5 MW and 100 kWh respectively is connected to Bus 3. The FESS is operated to assist Bus 3 and to store the surplus wind energy in the system if any. Recovery risk profile of different load points and the system while trying to recover the loss of a 0.2 p.u. generation capacity is shown in Figure 4.9. The FUC approach was used in the study. The wind speed was assumed to have the falling trend at the time of the major contingency. The risk profile is presented considering two different initial SOC of FESS plant at the time of the contingency. Since the FESS is operated to assist only Bus 3, the LPRR at other busses stays the same. The SRR from Figure 4.6 has been superimposed for reference. With the assistance from FESS plant, the risk profile at Bus 3 and system's recovery risk is seen to have significantly improved. The recovery risk in case of higher OWP is better contained when there is higher initial SOC of the FESS plant, as shown in the figure. The high SOC of the plant helps to absorb the disturbances more effectively while limiting the plant's ability to store the surplus wind in the system. The knowledge of historical wind pattern

and its diurnal characteristics thus become essential for the operator to set operating strategy of the FESS plant to have optimum SOC level of the plant at different times of the day for reducing wind spillage while maintaining the acceptable risk profile at the same time.

It is seen that in case of rising wind trend the risk profile does not degrade significantly and thus does not call for additional assistance from FESS. However, even under such scenario, FESS can be used simply to store the surplus wind to reduce the wind curtailment. Following study is carried out assuming the initial SOC of FESS to be 60% of rated capacity and considering the rising trend in the wind speed profile at the time of major contingency. Figure 4.10 shows the reduction in EWS due to the use of FESS to mitigate disturbances under different OWP levels. Since the surplus wind is captured by the FESS, the spillage drops significantly. Furthermore, the risk profile can be seen further reduced with the use of FESS.

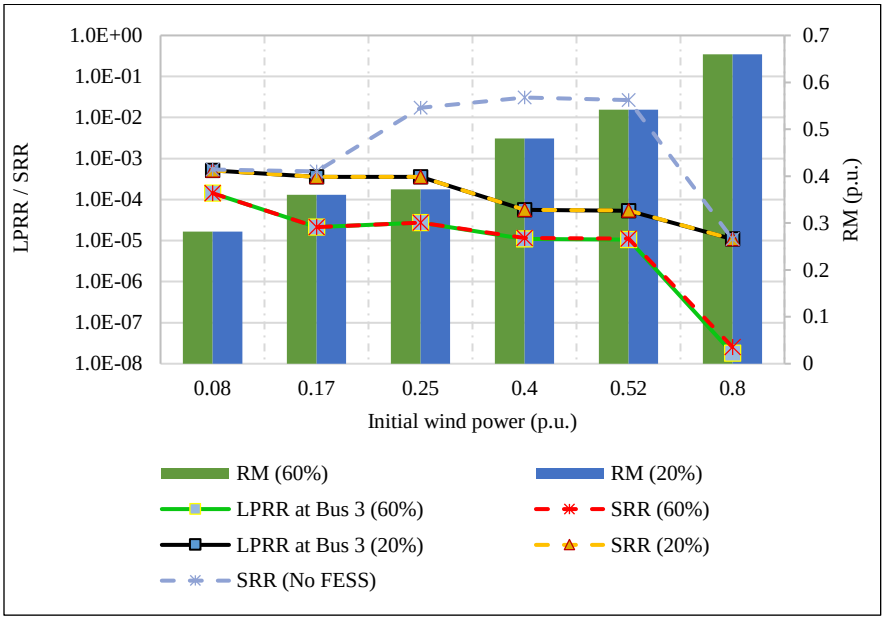

Figure 4. 9. Recovery risk profile with falling trend in wind speed at the time of major contingency considering assistance from FESS.

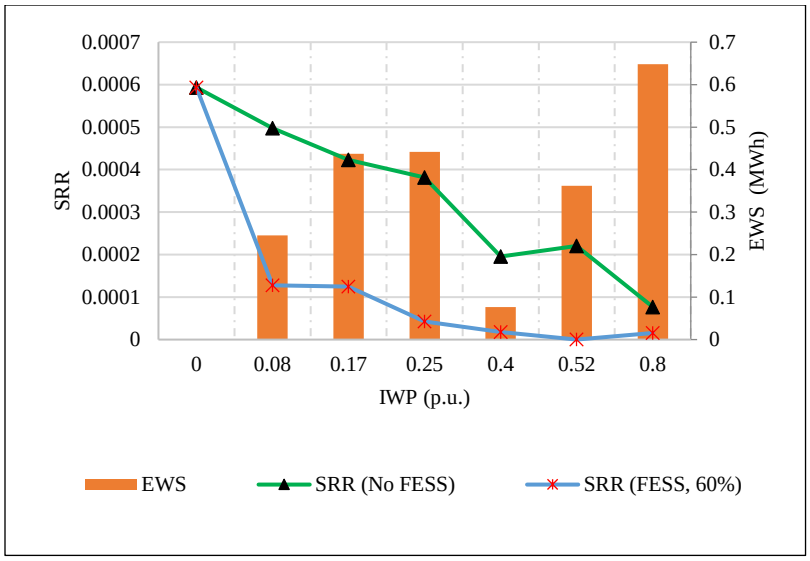

Figure 4. 10. Reduction of wind spillage and increment in SOC of FESS plant.

4.7. Conclusion

Modern power systems are exposed to higher operating risks owing to the large scale integration of highly intermittent energy sources such as wind. The energy storage systems that are capable of providing prompt assistance whenever needed, such as FESS, are essential to absorb the stochastic perturbations resulting from random loss of generation units, transmission line outage and wind power fluctuations. This paper proposes an analytical framework for operating risk assessment of wind-integrated composite power system using recovery risk analysis approach to quantify the reliability benefits of FESS in power system operation. The SRR and LPRR indices proposed in this paper are effective to establish the operating risk profile of the overall system and individual load delivery points respectively. The preliminary risk assessment carried out using the proposed framework without FESS, together with knowledge of historical wind speed pattern helps to determine the operating strategy of FESS. For a given major contingency disturbance, which could be loss of operating unit(s) or line(s), the system's ability to recover the pre-contingency supply-demand balance significantly depends upon the available SOC of FESS and wind speed profile at the time of the disturbance, in addition to the ramp rates of the healthy operating units. The recovery risk profile of the system as well as that of individual load points degrades with increasing operating wind penetration for the scenarios with falling trend at the time

of a major contingency disturbance. The degradation in the recovery risk profile becomes even worse with increasing operating wind penetration if prior knowledge of wind power is considered during unit commitment since doing so results in lower regulating energy being available from the committed firm capacity units. However, in such situations, the risk profile can be contained within acceptable range using FESS provided it has sufficient SOC at the time of the major disturbance. On the other hand, due to higher chances of having surplus wind energy to provide regulation, the risk profile actually improves with larger operating wind penetration for scenarios where wind speed is exhibiting rising trend at the time of the disturbance. FESS can be used under such scenarios too to boost up its SOC and also to reduce the wind spillage due to poor ramp-down rates of the available operating unit(s) and/or transmission line congestion. The proposed methods and indices can provide useful indicators to system operators in effectively integrating FESS to exploit renewable energy growth while maintaining acceptable operational reliability.

4.8. References

[1] Global Wind Energy Council, “Global wind statistics 2017.” pp. 1–4, 2017.

[2] North American Electric Reliability Corporation, "Reliability standards for the bulk electric systems of north america," NERC, Atlanta, GA, 2013.

[3] J. Cui, K. Li, Y. Sun, Z. Zou and Y. Ma, "Distributed energy storage system in wind power generation," *2011 4th International Conference on Electric Utility Deregulation and Restructuring and Power Technologies (DRPT)*, Weihai, Shandong, 2011, pp. 1535-1540.

[4] S. Rani Gongada, T. S. Rao, P. M. Rao and S. Salima, "Power system contingency ranking using fast decoupled load flow method," *2016 International Conference on Electrical, Electronics, and Optimization Techniques (ICEEOT)*, Chennai, 2016, pp. 4373-4376.

[5] Y. Jia, P. Wang, X. Han, J. Tian and C. Singh, "A Fast Contingency Screening Technique for Generation System Reliability Evaluation," in *IEEE Transactions on Power Systems*, vol. 28, no. 4, pp. 4127-4133, Nov. 2013.

[6] S. Fliscounakis, P. Panciatici, F. Capitanescu and L. Wehenkel, "Contingency Ranking With Respect to Overloads in Very Large Power Systems Taking Into Account Uncertainty, Preventive, and Corrective Actions," in *IEEE Transactions on Power Systems*, vol. 28, no. 4, pp. 4909-4917, Nov. 2013.

[7] S. Chen, Q. Chen, Q. Xia, H. Zhong, and C. Kang, 2015, “N− 1 security assessment approach based on the steady-state security distance”, *IET Generation, Transmission & Distribution*, *9*(15), pp.2419-2426

[8] T. Ding, C. Li, C. Yan, F. Li and Z. Bie, "A Bilevel Optimization Model for Risk Assessment and Contingency Ranking in Transmission System Reliability Evaluation," in *IEEE Transactions on Power Systems*, vol. 32, no. 5, pp. 3803-3813, Sept. 2017.

[9] R. Billinton, R. N. Allan, Reliability Evaluation of Power Systems, New York: Plenum, 1996.

[10] S. Thapa, “Operating risk analysis of wind integrated generation system,” Ph.D. dissertation, Univ. Saskatchewan, Saskatoon, 2014.

[11] P. Wang, Z. Gao and L. Bertling, "Operational Adequacy Studies of Power Systems With Wind Farms and Energy Storages," in *IEEE Transactions on Power Systems*, vol. 27, no. 4, pp. 2377-2384, Nov. 2012.

[12] Z. Parvini, A. Abbaspour, M. Fotuhi-Firuzabad and M. Moeini-Aghtaie, "Operational Reliability Studies of Power Systems in Presence of Energy Storage Systems," in *IEEE Transactions on Power Systems*, 2017.

[13] A. Alabdulwahab, A. Abusorrah, X. Zhang and M. Shahidehpour, "Coordination of Interdependent Natural Gas and Electricity Infrastructures for Firming the Variability of Wind Energy in Stochastic Day-Ahead Scheduling," in *IEEE Transactions on Sustainable Energy*, vol. 6, no. 2, pp. 606-615, April 2015.

[14] H. A. Sturges, "The choice of a class interval," *Journal of the American statistical association*, vol. 21, no. 153, pp. 65–66, 1926.

[15] [http://wind.nrel.gov/Web nrel/, accessed: July 2014.]

[16] S. Adhikari, R. Karki, "Reliability modelling of flywheel energy storage system for power system operational reliability assessment", presented at the SEEP Conf., May 2018

[17] C. Feinstein, P. Morris, and G. Hamm, "A review of reliability of electric distribution system components: EPRI white paper," *EPRI-1001873, California*, 2001.

[18] Dept. of Defense, MIL-HDBK-217F-Reliability Prediction of Electronic Equipment, Washington, D.C., December 2 1991.

[19] P. Upadhyay and N. Mohan, "Design and FE analysis of surface mounted permanent magnet motor/generator for high-speed modular flywheel energy storage systems," in *Energy Conversion Congress and Exposition, 2009. ECCE 2009. IEEE*. IEEE, 2009, pp. 3630–3633.

[20] F. Deiana, A. Serpi, J. Abrahamsson, I. Marongiu and G. Gatto, Extensive losses estimation of a novel high-speed permanent magnet synchronous machine for flywheel energy storage systems, *2016 XXII International Conference on Electrical Machines (ICEM)*, Lausanne, 2016, pp. 1728-1734.

[21] C. Zhang, K. J. Tseng, T. D. Nguyen and S. Zhang, "Design and loss analysis of a high speed flywheel energy storage system based on axial-flux flywheel-rotor electric machines," *2010 Conference Proceedings IPEC*, Singapore, 2010, pp. 886-891.

[22] D. M. Gay, "IBM ILOG CPLEX Optimization Studio Getting Started with CPLEX," 2011.

[23] R. Billinton, S. Kumar, N. Chowdhury, K. Chu, K. Debnath, L. Goel, E. Khan, P. Kos, G. Nourbakhsh and J. Adjei, "A reliability test system for educational purposes - basic data," *IEEE Trans. Power Syst.*, vol. 4, no. 3, pp. 1238–1244, 1989.

CHAPTER 5: SUMMARY AND CONCLUSIONS

Owing to the stochastic nature of power system operation, maintaining a reliable yet economic operation has always been a challenge to the power system operators. The power system's ability to cope with random outages and/or other unforeseen disturbances during the system operation is further restricted by addition of intermittent energy sources such as wind. The increasing adoption of renewable portfolio standard (RPS) by many countries projects a promising future of renewable energy sources in the generation mix. And with the projected growth rate in the usage of wind energy as electricity generation resource, the power system operators as well as planners are becoming increasingly concerned with the impacts of increasing RES penetration on reliable and economic operation of the power system.

Energy storage systems (ESS) can greatly reduce the generation variability and dampen the transmission line congestion thereby improving the operational reliability of the system. It is therefore various energy storage technologies are gaining importance, especially with the increased share of wind power and other RES in the generation mix. The suitability of different ESS technologies in the power system depends upon the inherent characteristics of the ESS itself. Pumped-hydro and compressed-air ESS are more suitable for long-term energy storage offering renewable capacity firming, load levelling and energy time shifts, while in situations when large chunk of power is needed immediately for short-duration, the ESS technologies with fast response such as FESS, batteries and ultra-capacitors are needed. Being a relatively less mature technology, the FESS is an expensive ESS. However, with recent advancement in power electronics, bearing system and rotor material, FESS is gaining popularity. Especially, the consistency in performance throughout its useful life (20 years on average), scalability due to compact modular designs, environmental friendliness, large DOD, low maintenance requirement makes FESS standout among other ESS technologies that are suitable from power system operational reliability perspective.

Operating reliability evaluation is an essential tool in real time decision making which can avoid widespread power outages and thus has great significance in power system operation. Due

to inability of conventional deterministic approach of reliability evaluation, in quantifying the actual risk associated with the operating condition, the regulating authorities responsible for enforcing the compliance standards are recommending to move toward risk based probabilistic approach. This approach considers the random failures of power system components during operation thereby capturing the stochastic nature of operating disturbances and thus outlines the true risk that the system is exposed to.

Unit commitment risk (UCR) and response risk (RR) are two major risk indices used in the literature as a tool to quantify the power system operational risk. UCR is concerned with determining number of units to be committed to meet the forecast load of known time while maintaining an acceptable probability of committed units being unable to meet the load. However, due to simplicity in use and understanding, utilities still choose N-1 criterion in practice as a tool for unit commitment. RR deals with ability of the participating units to respond to any disturbances that may arise during system operation. RR is thus more concerned with the allocation of spinning reserve within the committed units in any given time. With the increased uncertainty in the generation resource as well as load, RR analysis becomes very important since it forms the basis for exploring the potential resources to mitigate the increasing risks in the power system operation with increasing RES penetration. And as mentioned in introductory section of this thesis, the scope of research work in this thesis is limited to RR analysis.

Chapter 1 provides an introduction to power system reliability in general as well as from operating reliability point of view. The implications of increased wind penetration on power system operational reliability and the role of ESS, particularly FESS, in mitigating the operating risk is also presented in Chapter 1. Related literatures and objectives of the research are also presented in this chapter.

Chapter 2 is aimed at developing the reliability model of FESS suitable for power system operating risk assessment. The impacts of failure rates of critical components of FESS, and the length of mission time on SOC distribution of FESS are analyzed in Chapter 2. The usability of the developed model in assessing the potential of FESS in disturbance mitigation is demonstrated through illustrative examples.

In Chapter 3 a novel framework for response risk evaluation of wind-integrated power system has been introduced. The proposed framework makes an improvement over the conventional assumption that is usually made in response risk evaluation. Quantifying the

operational reliability benefits of using FESS in wind-integrated power system and also the impacts of increasing operating wind penetration on the power system operational reliability are the main objectives of Chapter 3. A short-term wind power model based on conditional probability approach has also been introduced in this chapter.

Chapter 4 works on the fundamental concept of generation response risk from hierarchical level I of the power system operating risk evaluation (as presented in Chapter 3) and tries to extend the concept to hierarchical level II. Analytical framework for operating risk assessment of bulk power system (BPS) in terms recovery risk analysis has been introduced in this chapter. The framework is suitable for quantifying the reliability benefits of FESS from operating risk perspective of BPS operation.

In conclusion, the thesis presents probabilistic frameworks and reliability model of FESS suitable for reliability evaluation of wind-integrated power system operation and successfully quantifies the reliability benefits of using FESS in wind-integrated power system operation. The short-term wind power model presented in this thesis captures the diurnal variability of wind speed. The model is found effective to reflect the impact of short-term wind speed variation in the system operating risk. Several case studies illustrating the applicability of proposed models and methodology are presented throughout the thesis and some important conclusions were drawn accordingly. For instance, increasing operating wind penetration does not necessarily degrades or improves the operating risk profile; the risk depends on the wind-speed profile at the time of major contingency and the extent of consideration of prior-knowledge of wind condition in unit commitment. Higher SOC of FESS at the time of major contingency disturbance allows to mitigate the disturbance better, but also increases the chances of wind-spillage should there be large amount of surplus wind in the system. This inference provides an important insight to the system operator / planner to strategize the FESS operation to maintain some optimum SOC level considering the wind speed profile at different times of day. In addition to the overall system's preparedness to cope with the major contingency disturbance within some definite time as measured by SRR, the actual operating risk that individual load delivery points are exposed to for the given major contingency under given operating condition is also quantified using LPRR. To sum up, the thesis addresses the operational reliability concerns due to system disturbances with growing wind penetrations, and the quantitative implications of implementing flywheel energy storage systems

to mitigate these concerns. The thesis provides methodology and indicators that will be valuable in developing operating policies for sustainable wind energy for the future.